UNIVERSITY OF NAPLES FEDERICO II

DOCTORATE
MOLECULAR MEDICINE AND MEDICAL BIOTECHNOLOGY

XXX CICLO

EGFR activation promotes a hypertrophic phenotype in NAGLU depleted cardiomyoblasts, depicting features of mucopolysaccharidosis IIIB

Tutor
Prof. Luigi Michele Pavone

Candidate
Patrizia Sarogni

COORDINATOR
Prof. Vittorio Enrico
Avvedimento

Academic Year 2016/2017

INDEX

ABSTRACT

Mucopolysaccharidosis (MPS) IIIB is a lysosomal storage disease due to the deficiency of the enzyme α-N-acetylglucosaminidase (NAGLU) required for heparan sulfate degradation. Since perturbation of lysosomal homeostasis represents an important cause of cardiomyocyte dysfunction in cardiovascular diseases, we generated a model of the MPS IIIB by silencing NAGLU gene expression in H9C2 rat cardiomyoblasts. NAGLU-depleted H9C2 exhibited accumulation of abnormal lysosomes and a hypertrophic phenotype. Through a phospho-receptor tyrosine kinase array, we found the specific activation of the epidermal growth factor receptor (EGFR) in NAGLU-depleted H9C2 compared to control cells. The pretreatment of NAGLU-depleted H9C2 with the specific EGFR inhibitor AG1478 caused the reduction of both lysosomal aberration and cellular hypertrophy. Similar results were obtained when NAGLU-depleted H9C2 were treated with PD98059, a selective inhibitor of MEK/ERK downstream targets of EGFR. Furthermore, we found increased phosphorylation levels of c-Src in NAGLU-depleted H9C2 where c-Src perturbation affected the hypertrophic response. However, c-Src phosphorylation remained unaffected after treatment of NAGLU-depleted H9C2 clones with AG1478, posing c-Src phosphorylation upstream EGFR activation. Finally, the heparin-binding EGF-like growth factor (HB-EGF) protein resulted to be up-regulated in NAGLU-depleted H9C2, and its silencing caused a reduction of the hypertrophic response. These results demonstrate that both c-Src and HB-EGF may contribute to the hypertrophic phenotype of NAGLU-depleted cardiomyoblasts by activating EGFR signaling, and suggest that the inhibition of EGFR pathway might represent an effective therapeutic strategy for the cure of MPS IIIB cardiac disease.

1. INTRODUCTION

1.1 Lysosomes and lysosomal storage diseases

Lysosomes are cytoplasmic cellular organelles found in all nucleated eukaryotic cells. They are delimited by a single-layer lipid membrane and have an acidic internal pH of 4.5-5.0 that is maintained by an adenosine triphosphate (ATP)-dependent proton pump. Morphologically, the lysosome is a highly heterogeneous organelle since the size, shape, and number per cell are variable depending on the cell type. It may be spheric, ovoid, or occasionally tubular in shape, and may vary between 0.1 to 2 μm in size. The primary cellular function of the lysosome is the degradation and recycling of several macromolecules, including nucleic acids, proteins, glycosaminoglycans (GAGs), oligosaccharides, sphingolipids, and other lipids. Proteins, which must be degraded into the lysosomes, are introduced into these organelles by means of various mechanisms involving endocytosis, autophagy and direct transport through the lysosomal membrane. The endosomal/lysosomal system (E/L), together with the ubiquitin-proteosome system (UPS) and autophagosome, represents an important metabolic center for substrates degradation, by influencing various cellular functions, signal transduction and the regulation of genes expression (Figure 1).

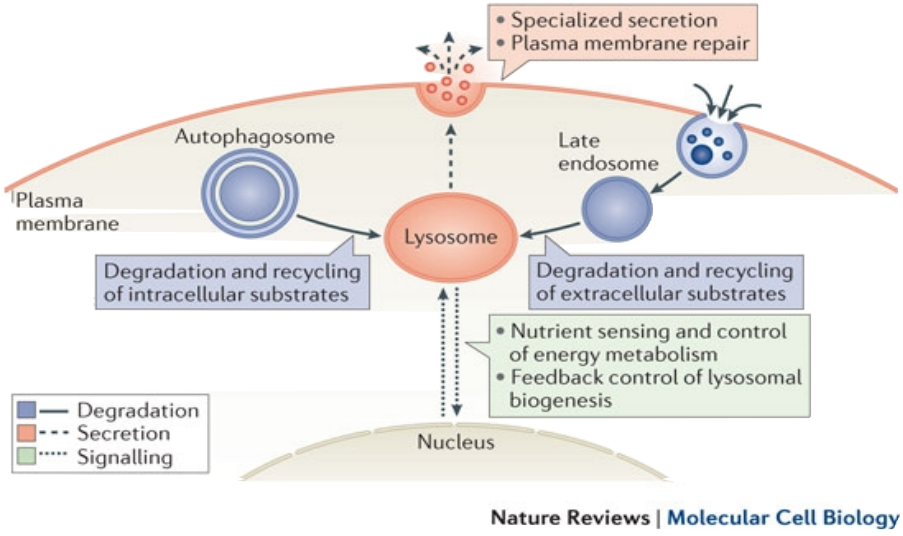

Figure 1. Main functions of the lysosome and their relationship with key cellular processes. *From Settembre C., et al. 2013. Nature*

Lysosomes are involved in a wide range of cellular processes, including cell signaling, antigen presentation, immunity, plasma membrane repair, or initiation of apoptosis. They are crucial for the maturation of phagosomes to phagolysosomes during phagocytosis, which is a fundamental mechanism during cellular pathogen defense. During exocytosis, lysosomes fuse with plasma membrane in response to increased concentration of cytosolic Ca^{2+} providing an extra membrane for wound repair (Reddy A. et al., 2001; Rodriguez A. et al., 1997). Lysosomal damage seems to be an early event in the apoptotic signaling cascade prior to increase the permeability of the mitochondrial membrane and the release of apoptogenic factors. Lysosome-mediated apoptosis also involves the lysosomal cathepsins. These proteolytic enzymes are able to cleave pro-apoptotic molecules and caspases, acting as mediators between lysosomes and mitochondria (Conus S. et al., 2008). Lysosomal cathepsins are also required for the generation of antigenic peptides from exogenous proteins, and are involved in the trafficking and maturation of the major histocompatibility complex (MHC) class II (Chapman H.A., 1998; Driessen C. et al., 1999), thus playing a role in adaptive immunity. In addition, intracellular cholesterol homeostasis is controlled through a lysosomal transporter, the Niemann-Pick, Type C1 protein (NPC1).

Lysosomal Storage Diseases (LSDs), with an incidence of 1/7000 birth, are genetic disorders caused by mutations in genes encoding for lysosomal enzymes or transporters. The deficeincy of these proteins results in the accumulation of one or more undegraded substrates in the lysosomes of different orgnas leading to cell death (Platt F.M and Walkley S.U., 2004) (Figure 2).

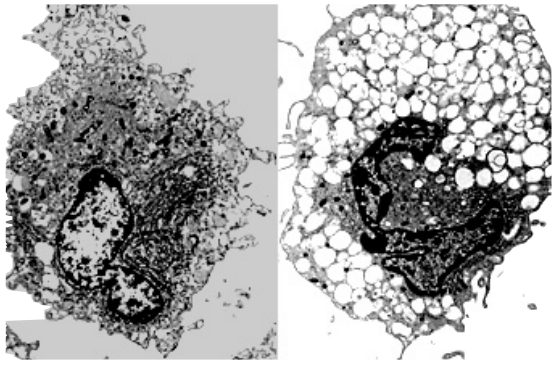

Figure 2: Lysosomes enlargement in MPS-affected mouse liver sections compared to a wilde-type mouse. *From Platt F.M., et al., 2004*

Although the cytotoxicity of the enlarged lysosomes is still considered the primary cause of the LSDs, recent studies have revealed new pathogenetic mechanisms (Walkley S.U et al., 2009). Among these, autophagy deregulation is considered the major causes of LSDs together with dysfunctions of the UPS system (Settembre C. et al., 2008). These evidences support the role of the lysosome as a central element between endocytic flows and metabolic recovery.

1.2 Glycosaminoglycans and their catabolism

Glycosaminoglycans (GAGs) or mucopolysaccharides are linear polysaccharidic chains formed by diacidic units of an exosamine (glucosamine or galactosamine) and an uronic acid (glucuronic or iduronic acid), with the exception of keratan sulfate in which the uronic acid is replaced by an hexose (galactose). The GAGs, based on the nature of the esosamine residues, are classified into two groups: 1) glucosaminoglycans which include hyaluronic acid (HA), keratan sulfate (KS), eparan sulfate (HS) and heparin; 2) galactosaminoglycans which comprise chondroitin sulfate (CS) and dermatan sulfate (DS) (Figure 3).

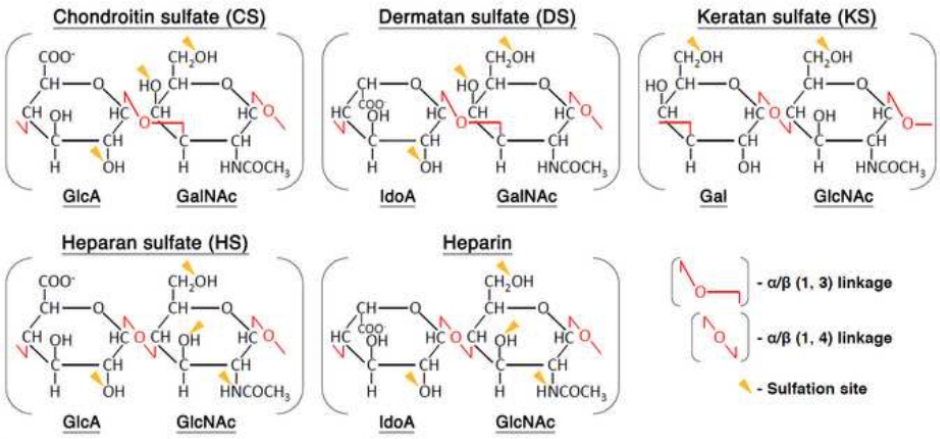

Figure 3: Structures of galactosaminoglycans and glucosaminoglycans. *From Deyan M., et al., 2015. JBC*

Monosaccharide units are bound together by a glycosidic bond between the hydroxyl group of the anomeric carbon (C-1) of a uronic acid and the hydroxyl group of an hexosamine, forming a long chain GAG. The high variety of these macromolecules is due to the presence of the sulfate groups on carbon atom 4 and 6 and the acetylation of the amino

group of the hexosamine. The molecular weight of the GAG ranges between 50,000 and 4,000,000 Dalton (Da). Due to the high content of carboxyl groups (-COO-) and esterified sulfate groups (-O-SO^{3-}), GAGs are polyanions wherein the number of negative charge per unit of disaccharide is 1 in the hyaluronic acid up to 4 in the heparin. Most of the fragments and monosaccharides generated by GAG degradation, occurring in the lysosomes, return in the cell biosynthetic pathways. The degradation process is finely regulated and mediated by hydrolytic enzymes that are substrate-specific, in accordance with sugar stereoisomers, with the type of the glycosidic bond, and with the pH of the lysosomal compartment. The first class of these enzymes includes esoglycosidases that catalyze the release of the specific monosaccharide at the non-reducing end of the oligosaccharide chain. The endoglycosidases, in turn, hydrolyze specific glucidic sequences within the biopolymer, generating fragments of about 10 kDa. Sulphatases, exosaminidases and glucuronidases also co-operate at the hydrolysis process (Table 1).

Enzyme	Reaction
Iduronate-2-sulfatase	Hydrolysis of the 2-sulfate group in L-iduronate of DS and HS
! -iduronidase	Hydrolysis of not sulfated iduronic bond in DS
GalNAc-4-sulphatase	Hydrolysis of 4-sulfate group of GalNAc4S and GalAGs
GalNAc-6-sulphatase	Hydrolysis of 6-sulfate group of GalNAc6S and D-gal
! -glucuronidase	Removal of residual of ! -GlcA

Table1: Lysosomal enzymes involved in degradation of GAGs.

GAGs are often associated to a protein core, giving rise to the proteoglycans (Figure 4), which constitute the major components of the extracellular matrix and of the connective tissue (Chaplin et al. 1986).

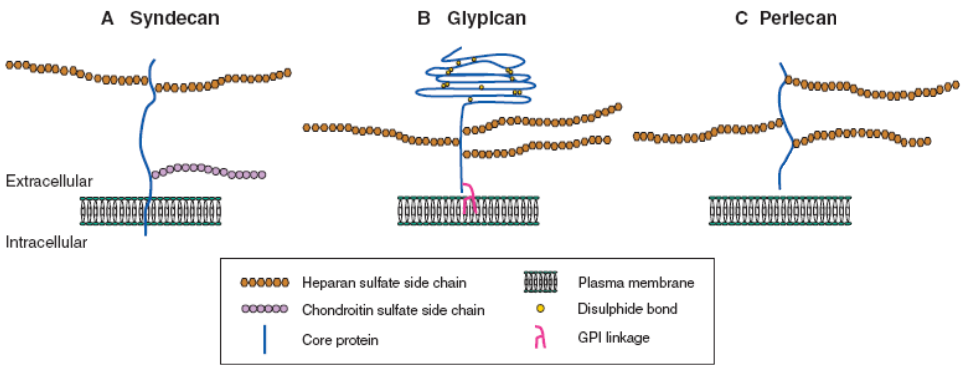

Figure 4: The three main classes of cell-surface heparan sulfate proteoglycans. *From Xinhua L., 2004. Development*

Proteoglycans participate in a plethora of cellular functions, both at the cell surface and intracellularly, and are thus indispensable for many essential processes including morphogenesis, neuronal development, tumor formation, and pathogen uptake (Mikami T. and Kitagawa H., 2013; Sarrazin S. et al., 2011).

1.3 Heparan sulfate proteoglycans (HSPGs)

HSPGs are the major determinants of how cells sense, integrate and respond to their environment. They mediate multiple biological processes as receptors or co-receptors for many protein ligands in the extracellular matrix (ECM) (Esko J.D. and Selleck S.B., 2002). HSPGs primarily regulate interactions between adjacent cells or between cells and the ECM, and they control cell adhesion, proliferation and migration. Importantly, HSPGs cooperate with integrins and the major class of ECM receptors to activate intracellular signaling cascade (Lopes C.C. et al., 2006) (Figure 5).

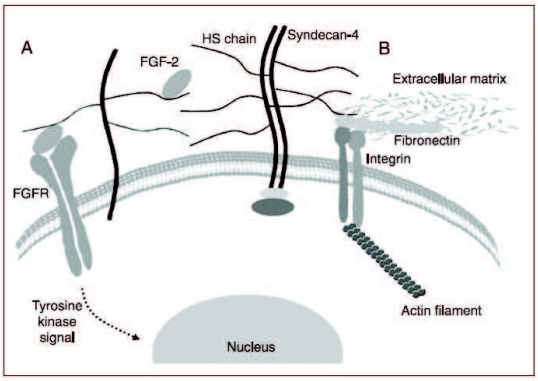

Figure 5: HSPGs-integrin cooperation. HSPGs modulate growth factor signaling (A) and participate in cell adhesion (B). (A) Formation of a ternary complex between HS, FGF and FGFR and subsequent signal transduction are represented. (B) Focal adhesion in which integrins and HSPGs cooperate to connect the ECM and the cytoskeleton is represented. *From Lopes et al., 2006.*

HSPGs ligands include ECM constituents (e.g. fibrin, fibronectin, laminin, and various types of collagen), cell adhesion molecules (L-selectin, N-CAM), and soluble growth factors (EGF, FGF, insulin-like growth factor-2, platelet-derived growth factor, transforming growth factor, vascular endothelial growth factor, hepatocyte growth factor). In addition, HS chains possess the ability to bind cytokines such as interleukin (IL)-5, IL-6, IL-8, IL-10, or tumor necrosis factor (TNF) (Whitelock J.M. and Iozzo R.V., 2005), playing a role in cytokine action regulation.

HSPGs have also important neurobiological functions. They play a role in the establishment and maintenance of neuronal connections and are therefore crucial for both CNS development and plasticity (Murrey H. and Hsieh-Wilson L.C., 2008). In neurons, extracellular HS regulates neural cell migration, axons growth and guidance, neuronal polarity and neurite outgrowth (Bovolenta P. and Fernaud-Espinosa I., 2000). These effects are mediated by growth factors (e.g., FGFs), secreted morphogens (e.g., Wnt or Shh), repellents and attractants (e.g. Slit, Netrin, or Semaphorins and Ephrins) (Hu H. et al., 2001; Lin L. et al., 2005).

Apart from sequestration of bioactive molecules, transmembrane (syndecans) and phospholipid-anchored (glypicans) HSPGs have a co-receptor role in which the proteoglycan, in concert with other cell surface molecules, comprises a functional receptor complex that binds the ligand and mediates its action (Kjellén L. and Lindahl U., 199). Cleavage of HS

side chains is therefore expected not only to alter the integrity of the ECM, but also to release HS-bound biological mediators. ECM-remodeling enzymes deeply affect cell and tissue functions. Heparanase is an endo-! -D-glucuronidase capable of cleaving HS side chains at a limited number of intrachain sites, yielding HS fragments of small size (~5-7 kDa) (Freeman C. and Parish C.R., 1998). Heparanase activity has long been detected in a number of cell types and tissues. Importantly, heparanase activity correlates with the metastatic potential of tumor-derived cells, attributed to enhanced cell dissemination as a consequence of HS cleavage and remodeling of the ECM barrier (Parish C.R. and Freeman C., 2001). In spite of its localization into a highly active protein degradation environment such as the lysosome, heparanase exhibits a halflife of about 30 hours (Gingis-Velitski S. and Zetser A., 2004). Residence and accumulation of heparanase in late endosomes and lysosomes may indicate that the enzyme acts in the physiological turnover of cellular HSPGs (Fuller M. and Chau A., 2005). Since the enzyme is not readily accessible to its extracellular substrate, regulatory mechanisms by which intracellular lysosomal heparanase is secreted in response to local or systemic stimuli should exist.

1.4 Mucopolysaccharidoses

Mucopolysaccharidoses (MPSs) are a group of lysosomal diseases caused by the lack of enzymes responsible for the catabolism of mucopolysaccharides (Neufeld E.F. and Muenzer J., 2001). MPSs are autosomal recessive disorders, with the exception of the MPS II which is transmitted as an X-linked tract. MPS I (Hurler Syndrome) is caused by the deficiency of the ! -L-iduronidase (IDUA) enzyme, whose gene cause the HS and DS lysosomal accumulation. The accumulation of the same metabolites is found in the MPS II (Hunter syndrome) caused by mutations in the idronate-2-sulphatase enzyme (IDS) gene. MPS III (Sanfilippo syndrome) is subdivided into 4 subtypes, depending on the missing enzyme: eparan-N-sulphatase (SGSH) in MPS IIIA (Sanfilippo syndrome type A), N-acetylglucosaminidase (NAGLU) in MPS IIIB (Sanfilippo syndrome type B), ! -glucosaminide-N-acetyltransferase (HGSNAT) in MPS IIIC (Sanfilippo syndrome type C), and N-acetylglucosamine-6-sulphatase (GNS) in MPS IIID (Sanfilippo syndrome type D). All these subtypes of MPS III are characterized by the HS lysosomal accumulation. MPS IV (Morquio syndrome) is divided into two subtypes: MPS IVA (Morquio syndrome type A) due to the deficiency of the N-acetylgalactosamine-6-sulfate sulphatase (GALNS) enzyme, and MPS IVB (Morquio syndrome type B) resulting from the

deficiency of ! -galactosidase (! -GAL). In both MPS IV subtypes the lysosomal accumulation products are CS and DS. MPS VI (Maroteaux-Lamy syndrome) is caused by the deficiency of the N-acetylglucosamine-4-sulphatase enzyme (arylsulfatase B, ARSB), whose gene encodes for a DS degradation enzyme. MPS VII (Sly syndrome), in which the lysosomal accumulation of HS and DS is detected, is caused by the lack of ! -D-glucuronidase (GUSB) enzyme. Finally, the most recently identified MPS IX is caused by hyaluronidase enzyme deficiency (HYAL1) and it is characterized by the lysosomal accumulation of hyaluronic acid, the only GAG that is not sulfated (Figure 6).

Disease	Protein deficiency	Chromosome location	Storage material
MPS I (Hurler, Scheie, Huler:Scheie)	α-L-iduronidase	4p16.3	HS/DS
MPS II (Hunter)	Iduronate-2-sulfate sulfatase	Xq27-28	HS/DS
MPS IIIA (Sanfilippo A)	Heparan N-sulfatase	17q25.3	HS
MPS IIIB (Sanfilippo B)	α-N-acetyl-glucosaminidase	17q21.1	HS
MPS IIIC (Sanfilippo C)	Acetyl-CoA:α-glucosaminide acetyltransferase	8p11-8q11	HS
MPS IIID (Sanfilippo D)	N-acetylglucosamine-6-sulfatase	12q14	HS
MPS IV A (Morquio A)	Galactose-6-sulfatase	16q24.3	KS
MPS IV B (Morquio B)	β-galactosidase	3p21-pter	KS
MPS VI (Maroteaux-Lamy)	Galactosamine-4-sulfatase	5q13-q14	DS
MPS VII (Sly)	β-glucuronidase	7q21-q22	DS/HS/CS

Figure 6: Classification of MPSs according to the missing enzyme and the lysosomal accumulated product.

MPSs exhibit a variable phenotype in both severity and progression, which include skeletal malformations, dimorphic facial features, organomegaly, and motor and neurological defects. In some forms, such as MPS I, MPS II and all subtypes of MPS III, mental retardation is the main clinical symptom and it is associated with a severe disability. Skeletal alterations, however, are typical of MPS IV and MPS VI.

Numerous studies *in vivo* have been carried out over the last years using the available animal models to explain the pathogenetic bases of MPSs. Like the other lysosomal diseases, many experimental trials have also demonstrated the involvement of an inflammatory response. The up-regulation of many proteins involved in inflammation, especially cytokines and proteases, has been demonstrated in animal models of MPS I (Ma X. et al, 2008; Metcalf J.A. et al., 2010), MPS VI (Simonaro C.M. et al, 2001-2005-2008-2010) and MPS VII (Simonaro C.M. et al, 2005-2008-2010; Richard et al., 2008; Metcalf J.A.et al., 2010). This up-regulation causes structural alterations in connective tissue/cartilage,

compromises elastogenicity and, finally results in skeletal and articular alterations. At least for MPS VI and VII, the up-regulation of the inflammatory response seems to be related to the activation of Toll-like receptor 4 signal transduction mechanisms (TLR4) (Simonaro C.M. et al, 2010). In MPS I and VII, alterations of the levels of the Fibroblast Growth Factor 2 (FGF2) and neurotropin have been decteted in vitro (Pan C. et al., 2005) and in vivo (Richard et al, 2008) and associated with the patogenesis of the diseases. Oxidative stress markers were observed in MPS I and II patients (Pereira V.G. et al., 2008; Hamano K. et al., 2008) and murine MPS I (Reolon G.K. et al, 2009). In addition, impairement of autophagy, with a lack of fusion between autophagosomes and lysosomes, has been demonstrated in the murine models of MPS IIIA and MPS VI as well as in another lysosomal disease like the Multiple Sulfate Deficiency (MSD) (Settembre C. et al., 2008; Ballabio A. et al., 2009). Other mechanisms may be involved in the pathogenesis of MPS: for example, it is known that the accumulation of unfolded or incorrectly folded protein usually generates endoplasmic reticulum (ER) stress resulting in a response characterized by changes in specific proteins, attenuation of translation, induction of ER chaperonins and degradation of non-folded proteins (Jellinger K.A. et al, 2009). In particular, cell homeostasis alterations that relate to the folding of proteins in the ER activate a signal transduction process known as the “Unfolded Protein Response” (UPR); initially cytoprotective, the UPR triggers an apoptotic cascade under conditions of prolonged or aggravated ER stress. ER stress is considered a possible cause of neurodegeneration in one of the most well known tauopathies, such as Alzheimer's disease, and in the lysosomal accumulation disorders (Hoozemans J.J. et al, 2009; Wei S.J. et al., 2008).

1.5 Mucopolysaccharidosis IIIB

Mucopolysaccharidosis IIIB (MPS IIIB) is a subtype of the MPS III caused by mutations in the gene encoding for the lysosomal enzyme NAGLU involved in the degradation of HS (Figure 7).

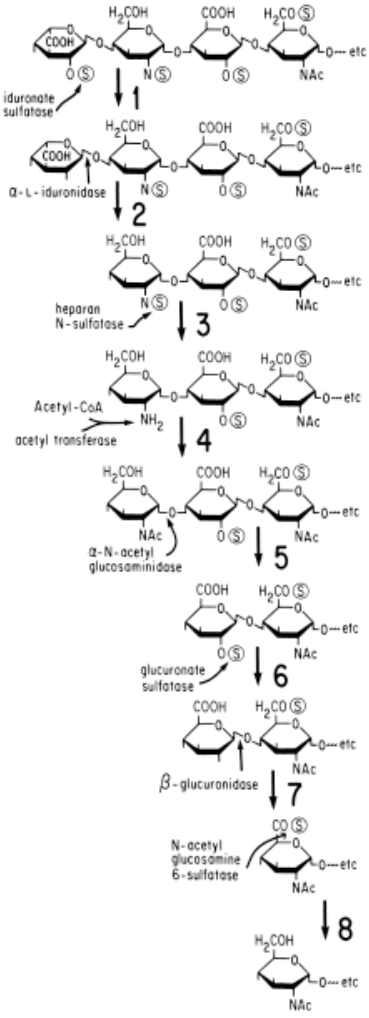

Figure 7: Heparan sulfate degradation pathway.

The disease has an incidence of 1 on 235,000 live births (Meikle P.J. et al., 1999) and it is characterized, from a clinical point of view, by a relatively mild somatic manifestation and by severe neurological disorders. The onset of clinical symptoms occurs between 2 and 6 years of age. Affected childrens, at birth seem appearently normal, but their

condition progressively worsen, and they develop serious neurological manifestations that include hyperactivity, aggressive behavior and sleep disorders, with rapid deterioration of social and adaptive abilities (Neufeld E.F. and Muenzer J., 2001). The neuropsychiatric abnormalities are divided into three phases (Cleary M.A. and Wraith J.E., 1993; Bax M.C. and Colville G.A., 1995): affected children between 1-4 years of age show only development delay, from 4 years onwards they show serious behavioral disorders, and, finally, physical deterioration and loss of strength. Life expectancy for subjects affected by the severe form of the disease is up to adolescence, although a higher survival characterizes patients with milder forms.

The NAGLU gene extends for 8.2 Kb from the site of initiation to the polyadenylation site, with 6 exons whose size ranges from 86 bp to 1452 bp. The cDNA encodes for a protein of 720 amino acids with 6 potential N-glycosylation sites (Zhao H.G. et al., 1996; Weber B. et al., 1996). NAGLU protein was firstly purified from placenta (Weber B. et al., 1996), liver (Sasaki T. et al., 1991) and urine (Salvatore D. et al., 1984), and its biosynthesis and maturation has been studied in skin fibroblasts (von Figura K. et al., 1984) and in human carcinoma cells (Di Natale P. et al., 1985). The molecular weight of the protein is 80-86 kDa for the precursor form, 77 kDa for the intermediate form and 73 kDa for the mature form. Recombinant NAGLU protein was expressed in CHO cells (Chinese Hamster Ovary cells), showing to be poorly phosphorylated in these cells (Yogalingam G. et al., 2000). The ineffective phosphorylation of the recombinant NAGLU protein in CHO cells does not allow its incorporation by MPS IIIB cells in vitro (Zhao K.W. and Neufeld E.F., 2000; Weber B. et al., 2001) and in vivo (Yu W.H. et al., 2000).

Regarding the pathogenesis of the MPS IIIB, many studies have been focused to understand the neuronal pathogenesis. In particular, it has been shown that the inflammatory process causes the activation of microglia and astrocytes and consequent secretion of cytokines and neurotoxic chemokines (Li H.H. et al, 2002; Ohmi K. et al., 2003; Villani G.R. et al., 2007) similarly to other neurodegenerative pathologies (Myerowitz R. et al, 2002; Wu Y.P. and Proia R.L., 2004). In one of the first murine model studies, the effect of HS accumulation on neuroplasticity has been analyzed (Li H.H. et al, 2002). Vitry and co-workers (2009) reported that lysosomal accumulation of HS-oligosaccharides in MPS IIIB neurons activates the synaptophysin proteasome degradation, a membrane protein of the synaptic vesicle related to synaptic potential, with consequences on components of these vesicles. More recently, the same group has suggested that the build up of vesicles, Golgi disorganization, and Golgi

biogenesis alterations may be involved in the dysfunction and neuronal death in MPS IIIB (Vitry et al., 2010).

1.6 The murine model of mucopolysaccharidosis IIIB

For the MPS IIIB, as for other MPS, a murine model ($NAGLU^{-/-}$) of the disease is available. It has been obtained by genetically modifying the exon 6 of the NAGLU gene (Li H.H. et al., 1999): a 852 bp fragment in the exon 6 has been replaced by an expression cassette containing Neomycin (NEO) gene. $NAGLU^{-/-}$ mice in the first months of life appear to be normal and healthy; both homozygous males and females are fertile up to six months of age and survive until 8-12 months of life. As they get older, $NAGLU^{-/-}$ mice become visibly ill, with weight loss, crawling hair, skin ulcers around the genital organs, and have difficulty in walking. The GAGs accumulate in the murine model, especially in the liver and kidney, in smaller amounts in the lung, spleen, thymus, heart, and brain, where there is also a secondary accumulation of gangliosides GM2 and GM3. In all organs, especially in the brain, the cells that most accumulate GAGs are those of the phagocytic system. 33 days after birth, vacuolate macrophages are found in many organs such as spleen, liver, lymphnodes, kidney, lung, skin, and brain. Neurons appear severely affected and various types of lesions are observed, especially in the cerebellum, in the Purkinje cells and in the cerebellar nuclei containing one or more inclusions visible with hematoxylin/eosin and with Shiff coloration. The murine model of MPS IIIB has sensory and behavioral deficits similar to that of human patients (Heldermon C.D. et al., 2007). Our research group recently demonstrated that $NAGLU^{-/-}$ mice also develop cardiac diseases and heart failure over time with dsyfunctions of the lysosomal-autophagic pathways (Schiattarella et al., 2015).

The disease in mice has a chronic and progressive course similar to that of human disease and, therefore, represents an excellent model for studying tthe pathogenesis of the MPS IIIB disease and to test new therapeutic approaches.

1.7 Therapies for mucopolysaccharidoses

There are limited treatments clinically available for MPSs. Symptomatic palliative therapies are readily available, but they only marginally improve the outcome of the disease. A classical therapeutic intervention consists of bone marrow transplantation (BMT). However, a high incidence of rejection limits the success of this treatment. For some MPSs, enzyme replacement therapy (ERT) is in clinical use, although ERT does not cross the blood-brain barrier and is ineffective on

neurological symptoms. In the recent years,gene therapy has been investigated, and the research group of Prof. P. Di Natale was the first one to demonstrate the efficacy of intravenous injection of a lentiviral vector containing the NAGLU gene as treatment for the MPS IIIB disease. With a single injection of this vector, the expression of the NAGLU transgene was detected in the liver, spleen, lung and heart of treated mice, and the recovery of enzymatic activity was obtained, resulting in the reduction of 55% of GAG content. This reduction remained unchanged for up of 6 months after treatment (Di Natale P. et al., 2005). Subsequently, the same group demonstrated that the intracranial injection of the lentiviral vector-NAGLU has the ability to alleviate many manifestations of the disease in MPS IIIB mice (Di Domenico C. et al., 2009). However, other studies have shown the efficacy of the use of adenoviral vectors (Heldermon C.D. et al., 2010). The substrate reduction therapy obtained by treatment with genistein is still under experimental phase for the MPS IIIB: while the first tests did not show any visible improvements, most recently, high doses of genistein for 9 months given to MPS IIIB mice seem to significantly reduce the lysosomal substate accumulation and neuro-inflammation in the cerebral cortex and in the hippocampus (Malinowska M. et al., 2009). However, studies are still in progress to identify new, alternative therapeutic approaches that might results to be more effective for the cure of MPS IIIB.

2. AIMS

In MPS diseases, the deficits of GAG degrading enzymes with the consequent substrate accumulation results in multiple organ dysfunctions, with distinct clinical manifestations depending on the type of the lacking enzyme and the accumulated substrate (Neufeld E.F., 2001). Although the most relevant clinical symptoms in affected patients include progressive neurodegeneration, behavior disorders, and skeletal abnormalities (Neufeld E.F., 2001), cardiac involvement has been also observed, and it accounts for the early mortality of these patients (Braunlin E. A. et al., 2011; Rigante D., 2002). Cardiac causes of death include heart failure, arrhythmias, coronary occlusion, pulmonary hypertension, and other cardiovascular dysfunctions. Among MPS subtypes, MPS IIIB is an autosomal recessive disorder caused by the deficiency of α-N-acetylglucosaminidase (NAGLU) involved in HS degradation. The availability of MPS IIIB animal models (Li H.H. et al., 1999; Ellinwood N.M. et al., 2003) and cultured cell systems (Yogalingam G. et al., 2011; Lemonnier T. et al. 2011), including primary fibroblasts from MPS IIIB patients, has provided definite evidence that the defective lysosomal clearance of undigested HS is the primary cause of organ dysfunctions observed in the patients.

Since an alteration of lysosomal homeostasis is an important cause of cardiomyocyte dysfunction in different cardiovascular diseases (Schiattarella G. et al., 2015), our research group previously investigated cardiac involvement in the MPS IIIB murine model. We demonstrated that NAGLU knock out mice develop heart disease, valvular abnormalities and heart failure (Schiattarella G. et al., 2015). Our study also highlighted that the cardiac defects observed in the NAGLU knock out mice correlate with an altered autophagic flux in the heart tissues. These findings prompted us to further investigate the mechanisms governing cardiac dysfunction in MPS IIIB. Indeed, a better understanding of the cellular and molecular mechanisms consequent to HS storage defects could be very useful to identify novel therapeutic targets for MPS IIIB.

The objective of my PhD project was to elucidate the link between abnormal lysosomal HS storage and the cardiac hypertrophic phenotype previously observed in the MPS IIIB mouse model. The investigation was carried out by generating a cellular model of the MPS IIIB through NAGLU gene silencing in H9C2 rat cardiomyoblasts. These cells have been proved to represent a relevant model to investigate mechanisms and consequences of cardiac pathologies, including hypertrophy (Watkins S.

J. et al., 2011), and differentiation (Ménard G. et al., 1999; Karagiannis T.C et al., 2010). A phospho-receptor tyrosine kinase (RTK) array allowed us to identify an activated epidermal growth factor receptor (EGFR) on NAGLU silenced H9C2 stable clones. Overall, the results of this study unraveled how pertubations in the EGFR signaling pathways account for cellular defects that are relevant to MPS IIIB pathophysiology, thus providing new insights into the molecular mechanism by which NAGLU silencing and consequent lysosomal impairment cause cardiac defects in MPS IIIB disease.

3. MATHERIALS AND METHODS

3.1 Antibodies and chemicals.

The rabbit anti-LAMP-2 polyclonal antibody (PA1-655) was purchased from Thermo-Fisher; mouse anti-diphosphorylated ERK1/2 monoclonal antibody (M8159) from Sigma Aldrich; rabbit anti-ERK1/2 polyclonal antibody (V114A) from Promega; rabbit anti-HB-EGF monoclonal antibody (ab185555) and rabbit anti-NAGLU monoclonal antibody (ab214671) from Abcam; rabbit anti-phospho-Src (Tyr416) polyclonal antibody (2101), rabbit anti-Src monoclonal antibody (2109), rabbit anti-phospho-EGFR (Tyr1173) monoclonal antibody (4407), and rabbit anti-EGFR monoclonal antibody (2646) from Cell Signaling Technology); mouse anti-beta-actin monoclonal antibody (G043) from Abm: goat anti-mouse IgG polyclonal antibody conjugated to horseradish peroxidase (HRP) (sc-2031) and goat anti-rabbit IgG-HRP polyclonal antibody (sc-3837) from Santa Cruz Biotechnology.

Nuclear 4′,6-diamidino-2- phenylindole (DAPI), bovine serum albumin (BSA), phalloidin, and the EGFR inhibitor AG1478 [N-(3-chlorophenyl)-6,7-dimethoxy-4-quinazolinamine] were purchased from Sigma Aldrich; SDS-PAGE reagents (Bio-Rad); the MEK inhibitor PD98059 [2-(2′-amino-3′- methoxyphenyl)-oxanaphthalen-4-one] from Calbiochem; ; fetal bovine serum (FBS) from GIBCO; LysoTracker from Thermo Fisher; IBAfect reagent (7-2005-050) from IBA BioTAGnology; 4-methylumbelliferyl-Nacetyl-α- D-glucosaminide from, Calbiochem; Trizol reagent from Invitrogen.

3.2 Cell cultures.

H9C2 rat cardiomyoblasts (ATCC) were cultured in Dulbecco's minimal essential medium (DMEM), 1g/L low glucose, 2 mM L-glutamine, 1 mM sodium pyruvate, supplemented with 10% FBS, 100 Units/ml penicillin, and 10 mg/ml streptomycin, at 37°C in a humidified 5% CO2 atmosphere.

For stable transfection, H9C2 cardiomyoblasts were plated at a density of 5×10^5 cells/100-mm tissue culture dish in antibiotic-free DMEM containing 10% FBS. and incubated for 24 h at 37°C with 5% CO2. Confluent cells were transfected, using IBAfect reagent, with a pool of plasmids codifying for three shRNAs (188A12, 566F3, 526A3, Open Biosystems) targeting NAGLU or with a control plasmid codifying for a non- targeting shRNA. After 48 h, transfected H9C2 were selected in the presence of 0.4 μg/ml of puromycin. Enzymatic activity assay and RT-PCR analysis were performed to identify the stable NAGLU-silenced

clones. Stable clones were grown in DMEM supplemented with 0.4 μg/ml of puromycin.

For transient transfections, H9C2 clones were plated at 2.5×10^5 cells/60-mm tissue culture dish 24 h prior to transfection. Transfections with plasmid vectors codifying for dominant negative (DN) and wild type (WT) c-Src, and control vector-GFP, kindly provided by Prof. A. Feliciello (University of Naples Federico II, Naples, Italy) (Cardone L., et al., 2004), were carried out using IBAfect reagent according to the manufacturer's instructions. Transient transfections of H9C2 clones with HB-EGF siRNA siRNAID 48748, Thermo-Fisher) and with a non-targeting siRNA were carried out using Lipofectamine RNAiMAX (Thermo-Fisher) according to the manufacturer's instructions.

3.3 Enzyme activity assay.

In order to evaluate NAGLU enzymatic activity in stable clones, pellets from 5×10^5 cells of each clone were collected, submitted to 10 freeze thaw cycles, and clarified by centrifugation. The protein concentration of samples was measured by the Lowry method, while NAGLU enzymatic activity was measured as described by Marsh and Fensom (1985) using 4-methylumbelliferyl-Nacetyl-α-D-glucosaminide as a fluorogenic substrate. Enzymatic activity was normalized for total protein concentration and hydrolysis of 1 nmol of substrate per hour per milligram of protein was defined as one catalytic unit.

3.4 Fluorescence microscopy.

LysoTracker was used to label lysosomes (Chazotte B., 2011). Briefly, live-cell clones grown on a coverslip were incubated with LysoTracker probe for 1 h at 37 °C, washed with PBS, and fixed with 4% paraformaldehyde (PFA) solution in PBS. After washing with PBS, the coverslips were mounted with 1:1 PBS/glycerol solution, and observed under a confocal fluorescence microscope. Phalloidin was used to label cytoskeleton. After washing with PBS, cells were fixed with 4% PFA solution in PBS. After washing, cells were permeabilized with 0.1% Triton X-100 in PBS and then stained with 50 μg/ml fluorescent phalloidin conjugate, phalloidin-TRITC, in PBS for 1 h at room temperature. Then, nuclei were counterstained with DAPI for 1 h. After washing, the coverslips were mounted with 1:1 PBS/glycerol solution, and observed under a confocal fluorescence microscope. Images were collected by a laser-scanning microscope (LSM 510 META, Carl Zeiss Microimaging, Inc.) equipped with a planapo 63x oil immersion (NA 1.4) objective lens.

3.5 Coomassie staining.

Cells of each clone were washed in PBS, fixed with 4 % PFA solution in PBS for 1 h at room temperature, washed in PBS, and stained with Coomassie brilliant blue solution for 1 h at room temperature. Then, the cells were washed in distilled water, dried for 24 h, observed under a white light microscope, and photographed by a Nikon camera.

3.6 Quantitative RT-PCR.

Total RNA from H9C2 clones was extracted using Trizol reagent. 500 ng of RNA were reverse transcribed for cDNA synthesis with Iscript RT-PCR system (Biorad). Reverse transcription of RNAs was followed by quantitative real-time polymerase chain reaction performed with the SYBR Green real time PCR master mix kit (FS Universal SYBR Green MasterRox/Roche Applied Science). The reactions were visualized by SYBR Green analysis (Applied Biosystem) on StepOne instrument (Applied Biosystem). Primers for gene analysis were the following:

ANP-Forward: 5'-GGAGCAAATCC CGTATACAGTGCG-3'
ANP-Reverse: 5'-GCGGAGGCATGACCTCATCTTCTAC-3'
BNP-Forward: 5'-CTGGGAAGTCCTAGCCAGTCTC-3'
BNP-Reverse: 5'CCGGAAGGCGCTGTCTTGAGACC-3'
MLC2V-Forward: 5'-GACCCAGATCCAGGAGTTCAAGG-3'
MLC2V-Reverse: 5'-CGAGGGCAGCAAACGTGTCCC-3'
NAGLU-Forward: 5'-GGCCAGGAGGCCATCTGGC-3'
NAGLU-Reverse: 5'-CCCAGGCCAGGAAGGCAGG-3'
S18-Forward: 5'-AAACGGCTACCACATCCAAG-3'
S18-Reverse: 5'CCTCCAATGGATCCTCGTTAA-3'
HB-EGF-Forward: 5'-GGACTACTGCATCCACGGAGAGT-3'
HB-EGF-Reverse: 5'-CCACCACAGCCAAGACGGTAGT-3'.

All standards and samples were assayed in triplicate. Thermal cycling was initiated with an initial denaturation at 95°C for 5 min. After this initial step, 40 cycles of PCR were performed. Each PCR cycle consisted of heating at 95°C for 30 sec for melting, 55°C for 30 sec for annealing and 72°C for 30 sec for the extension. To calculate the relative expression levels, we used the 2-ΔΔCT method (Livak K.J., et al., 2001).

3.7 Western Blotting.

Cells were harvested in lysis buffer containing 50 mM Tris ph7.5, 150 mM NaCl, 1 mM EDTA, 1 mM EGTA, 10% glycerol, 1% Triton-X-100, 1 mM ß-glycerophosphate, 1 mM phenylmethylsulfonyl fluoride, protease inhibitor cocktail tablet, 1 mM sodium orthovanadate, and 2.5

mM sodium pyrophosphate. The lysates were incubated for 30 min on ice, supernatants were collected and centrifuged for 10 min at 14,000 g. Protein concentration of protein extracts was measured by the Bradford assay. 25 or 50 µg/lane of total proteins were separated on SDS gels and transferred to nitrocellulose membranes. Membranes were treated with a blocking buffer (25 mM Tris, pH 7.4, 200 mM NaCl, 0.5% Triton X-100) containing 5% non-fat powdered milk for 1 h at room temperature. Incubation with the primary antibody was carried out overnight at 4 °C. After washings, membranes were incubated with the horseradish peroxidase- conjugated secondary antibody for 1 h at room temperature. Following further washings of the membranes, chemiluminescence was generated by ECL system. Densitometric analyses were performed using the NIH Image software (Bethesda, MD, USA).

3.8 Phospho-Receptor Tyrosine Kinase (Phospho-RTK) Array.

The phospho-RTK array (ARY001B, R&D Systems) which screens 49 RTKs, was performed as following described. All reagents and samples were prepared according to manufacturer's instructions. 2.0 ml of array buffer 1 was pipetted into each well of the 4-well multi-dish as a blocking buffer; each array was placed into each well of the 4-well multi-dish and incubated for 1 h at room temperature on a rocking platform shaker. Samples were prepared by diluting the desired quantity (50 µg of proteins) of cell lysates to a final volume of 1.5 ml with array buffer 1, and incubated overnight at 2-8°C on a rocking platform shaker pre-blocked membranes. Each array was carefully placed into individual plastic containers with 20 ml of 1X washing buffer, and the 4-well multi-dish was rinsed with deionized or distilled water and dried thoroughly. Each array was washed with 1X washing buffer for 10 min on a rocking platform shaker for three times. The anti-phospho-tyrosine-HRP detection antibody was finally diluted in 1X array buffer 2, and added to each array for 2 h at room temperature on a rocking platform shaker. Each array was washed three times with 2 ml of 1X washing buffer for 10 min on a rocking platform shaker. Membranes were incubated with 1 ml of the prepared Chemi Reagent Mix for 1 min. Membranes were exposed with an autoradiography film cassette to an X-ray film for 1-10 min. For the data analysis, the positive signal, seen on the developed film, was identified by placing the transparency overlay template on the array image and aligning it with the pairs of reference spots in the three corners of each array. Reference spots were included to align the transparency overlay template and to demonstrate that the array has been incubated with anti-phospho-tyrosine-HRP during the assay procedure.

3.9 Statistical Analysis.

The data reported are expressed as the mean ± standard deviation (S.D.) of at least three independent experiments of equal design. Statistical significance was assessed by Student's t-test. A value of $P < 0.05$ was considered to be statistically significant.

4. RESULTS

4.1 NAGLU depletion causes lysosomal defects in H9C2 cardiomyoblasts.

To study the molecular mechanisms underlying the cardiac disease in MPS IIIB, we generated a cellular model of the disease in H9C2 cardiomyoblasts by silencing NAGLU gene expression through a pool of three DNA plasmids carrying different sh-RNAs against NAGLU mRNA. Silenced clones (H9C2sh-NAGLU) showed a significant (70%) reduction of NAGLU catalytic activity compared to that of H9C2 stably transfected with a non-targeting sh-RNA (H9C2sh-CTR) (Figure 8).

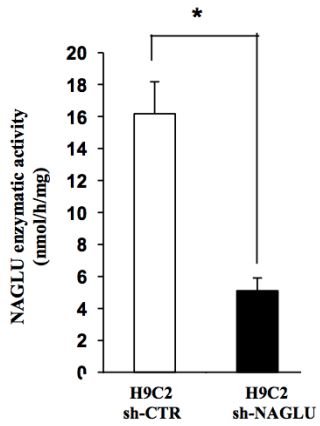

Figure 8: Reduction of NAGLU enzymatic activity in H9C2 stable silenced clones. NAGLU enzymatic activity in the extracts from selected NAGLU-depleted H9C2 stable clones (H9C2sh-NAGLU) and control H9C2 stably transfected with a non-targeting sh-RNA (H9C2sh-CTR). Cell lysates were assayed for protein content and enzyme activity as described in Materials and Methods. *P<0.05.

Accordingly, silenced clones (H9C2sh-NAGLU) showed a significant reduction of NAGLU mRNA and protein levels compared to that of H9C2sh-CTR clones (Figures 9).

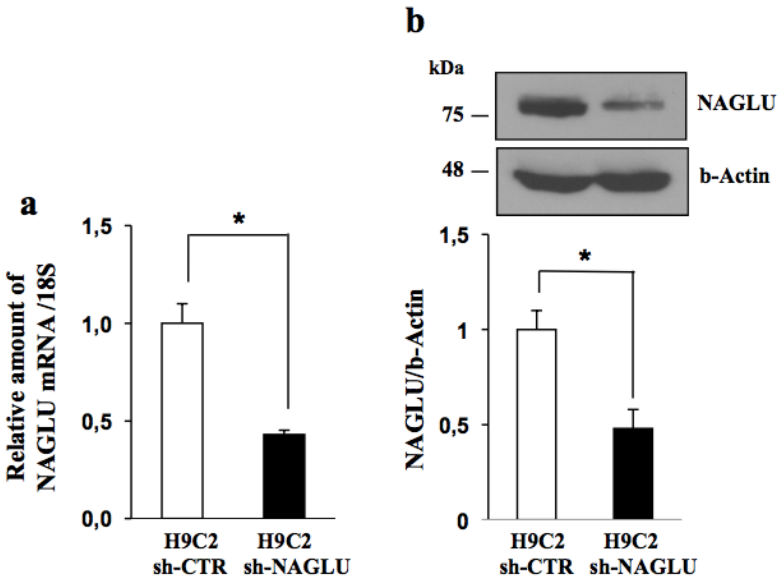

Figure 9: Reduction of NAGLU mRNA and protein levels in silenced stable clones. (a) NAGLU mRNA expression levels in H9C2sh-NAGLU and H9C2sh-CTR as measured by quantitative RT-PCR analysis. The amount of NAGLU mRNA was normalized with respect to the amount of 18S ribosomal RNA housekeeping gene. The data reported are the mean ± S.D. of 3 independent experiments. *P<0.05. **(b)** NAGLU protein levels in H9C2sh-CTR and H9C2sh-NAGLU as measured by Western blotting analysis. To monitor equal loading of protein, the blot was probed using anti-! -actin antibody. The data reported are the mean ± SD of three independent experiments of equal design. Densitometric analysis was performed, and the data obtained are reported on the histogram below. *P<0.05.

In MPS IIIB, the lack of NAGLU causes lysosomal accumulation of undegraded HS with consequent lysosomal enlargement. Therefore, we explored whether NAGLU silencing in H9C2 cardiomyoblasts induces aberrant lysosomal substrate accumulation. Staining with the LysoTracker probe showed more abundant and larger intracellular vacuoles in NAGLU-depleted H9C2 compared to H9C2sh-CTR (Figure 10a). Furthermore,, Western blotting analysis of the lysosomal associated membrane protein LAMP2 (Carlsson S.R.,et al., 1990) showed a

significant increase of LAMP2 protein levels in H9C2sh-NAGLU compared to H9C2sh-CTR (Figure 10b).

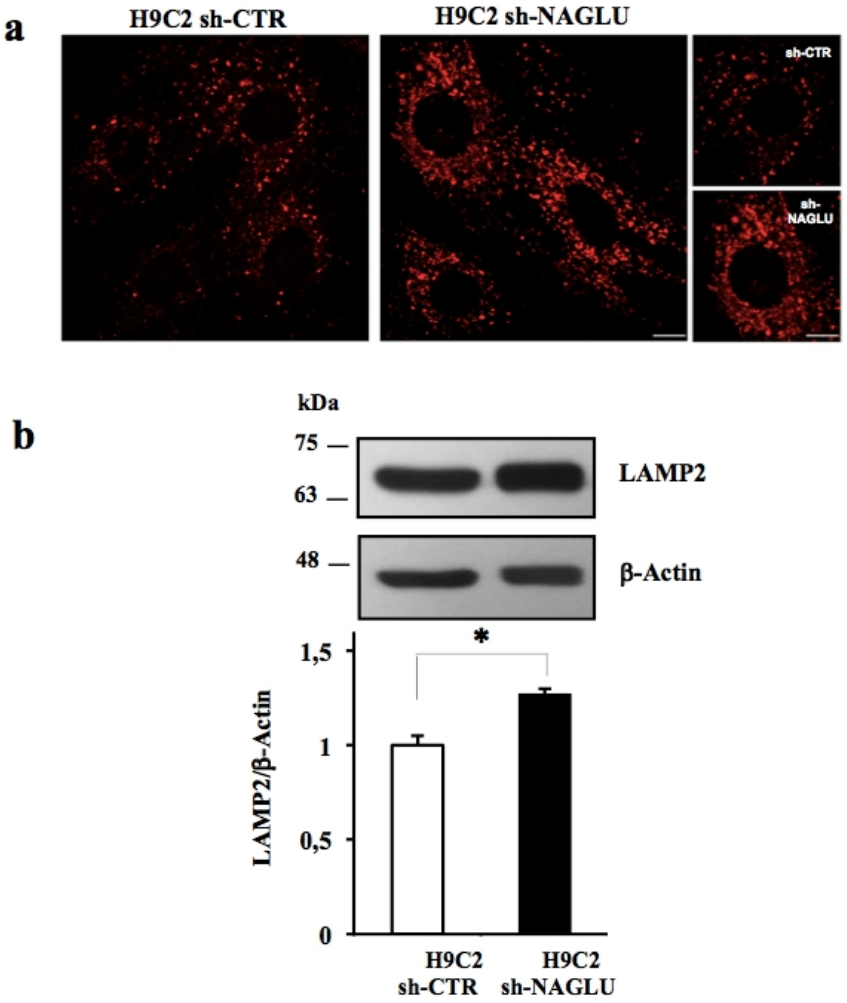

Figure 10: Lysosomal pathology in NAGLU silenced H9C2 cardiomyoblasts. (a) Fluorescent staining of lysosomes in H9C2sh-NAGLU and H9C2sh-CTR labeled by LysoTracker probe. In NAGLU-depleted H9C2 more abundant and larger intracellular vacuoles than control H9C2 are visible. **(b)** LAMP2 protein expression levels in H9C2sh-NAGLU and H9C2sh-CTR as measured by Western blotting analysis. The amount of LAMP2 as measured by densitometry was normalized with respect to the amount of ß-actin. The data reported on the

histogram below are the mean ± S.D. of three independent experiments. *P<0.05.

Furthermore, the staining with a fluorescent lectin that detecting sugars and glycoproteins containing β(1→4)-N-acetyl-D-glucosamine recognizes HS showed a more abundant intracellular and extracellular HS in the H9C2sh-NAGLU clones compared to H9C2sh-CTR where the main staining was observed exclusively in the Golgi apparatus (Figure 11).

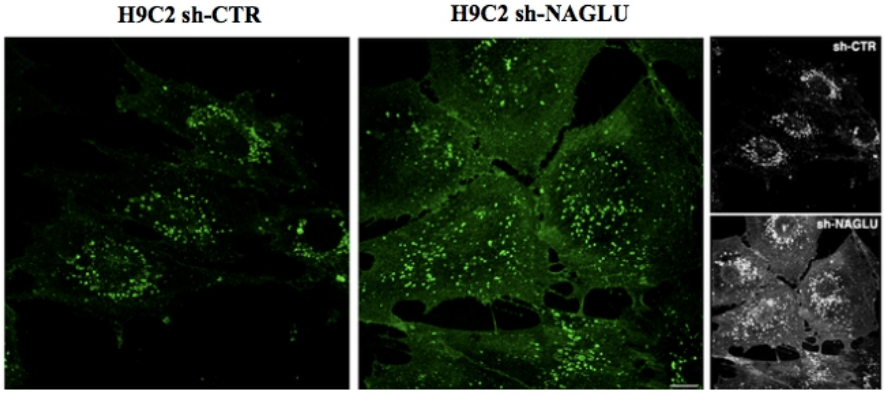

Figure 11. Intracellular and extracellular accumulation of HS in NAGLU silenced H9C2 cardiomyoblasts. Fluorescent staining of HS in H9C2sh-CTR and H9C2sh-NAGLU labeled by lectin-FITC. Scale bars 10! m. In NAGLU-depleted H9C2 an increased accumulation of HS on the cell membrane and in the periphery of the cells is detectable compared to control H9C2 clones.

Overall, these data demonstrate that H9C2sh-NAGLU cardiomyoblasts show the HS storage abnormalities observed in MPS IIIB, thus suggesting that this cellular model represents a valuable tool to investigate the pathogenesis of cardiac disease in MPS IIIB.

4.2 NAGLU depletion induces hypertrophy in H9C2 cardiomyoblasts.

Firstly, we asked whether the loss of NAGLU might cause cellular hypertrophy in H9C2 cardiomyoblasts as already detected in NAGLU knockout mice (Schiattarella G.G., et al. 2015). To this purpose, the cellular cytoskeleton of H9C2sh-NAGLU and H9C2sh-CTR was labeled with fluorescent phalloidin. H9C2sh-NAGLU showed a morphological

expansion which is typical of an hypertrophic phenotype (Figure 12a), as also detected when clones were stained with Coomassie blue (Figure 12b).

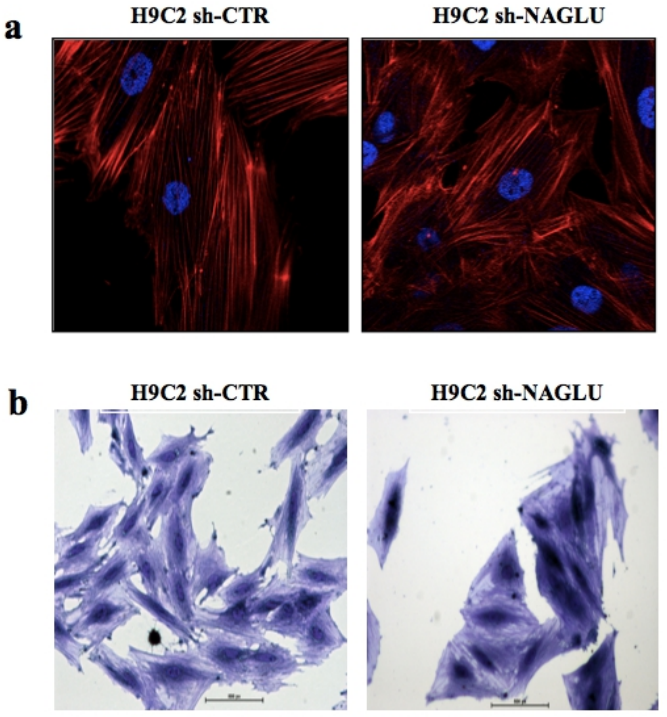

Figure 12. Hypertrophic phenotype of NAGLU silenced H9C2 cardiomyoblasts. **(a)** Phalloidin staining of H9C2sh-CTR and H9C2sh-NAGLU cellular cytoskeleton. Nuclei were counterstained with DAPI. Scale bars 10! m. Cell size enlargement was observed in NAGLU-depleted H9C2 compared control H9C2. **(b)** Comassie staining shows cellular hypertrophy. Pictures are representative of three indipendent experiments.

The hypertrophic phenotype of H9C2sh-NAGLU was further confirmed by analyzing the expression of two markers of hypertrophy: atrial natriuretic peptide (ANP) and brain natriuretic peptide (BNP) (Schiattarella G.G., et al. 2015). ANP and BNP mRNA levels were

significantly higher in H9C2sh-NAGLU than in control clones (Figure 13).

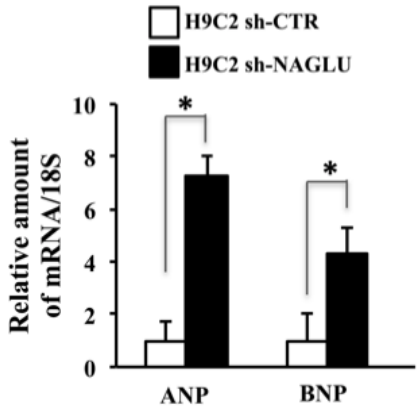

Figure 13: Expression levels of mRNAs coding for ANP and BNP hypertrophic mediators in H9C2sh-CTR and H9C2sh-NAGLU. The amount of ANP and BNP mRNA as measured by quantitative RT-PCR analysis was normalized with respect to the amount of 18S ribosomal RNA housekeeping gene. *P<0.05.

The differentiation capability under 1% FBS stimulation of H9C2 cardiomyoblasts into cardiomyocytes was impaired as measured by MLC2v mRNA levels (Figure 14). All together these data indicate that the loss of NAGLU leads to cellular hypertrophy and differentiation defects. In addition, these results confirm the reliability of our MPS IIIB cell model to investigate the molecular events induced by NAGLU silencing in cardiac cells.

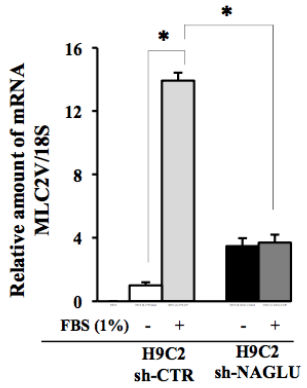

Figure 14. Impaired differentiation capability of NAGLU silenced H9C2 cardiomyoblasts. Expression levels of MLC2v mRNA in the presence and absence of FBS in H9C2sh-CTR and H9C2sh-NAGLU clones as detected by quantitative PCR. *P<0.05.

4.3 EGFR activation accounts for hypertrophy in NAGLU-depleted H9C2 cardiomyioblasts.

In order to investigate the molecular mechanisms responsible for lysosomal abnormalities and hypertrophic response induced by NAGLU silencing in H9C2 cardyomyoblasts, we performed a phospho- receptor tyrosine kinase (RTK) array on NAGLU-depleted H9C2 and H9C2sh-CTR. Among 49 tested RTKs (Table 2), we detected the specific phosphorylation of EGFR in H9C2sh-NAGLU (Figure 15a). Similar result was obtained by Western blotting analysis of the phosphorylation levels of EGFR in NAGLU-depleted H9C2 that resulted to be significantly higher than control cells (Figure 15b).

Coordinate	Receptor Family	RTK/Control	Coodinate	Receptor Family	RTK/Control
A1, A2	Reference Spots	___	D1, D2	Tie	Tie-2
A23, A24	Reference Spots	___	D3, D4	NGF R	TrkA
B1, B2	EGF R	EGF R	D5, D6	NGF R	TrkB
B3, B4	EGF R	ErbB2	D7, D8	NGF R	TrkC
B5, B6	EGF R	ErbB3	D9, D10	VEGF R	VEGF R1
B7, B8	EGF R	ErbB4	D11, D12	VEGF R	VEGF R2
B9, B10	FGF R	FGF R1	D13, D14	VEGF R	VEGF R3
B11, B12	FGF R	FGF R2α	D15, D16	MuSK	MuSK
B13, B14	FGF R	FGF R3	D17, D18	Eph R	EphA1
B15, B16	FGF R	FGF R4	D19, D20	Eph R	EphA2
B17, B18	Insulin R	Insulin R	D21, D22	Eph R	EphA3
B19, B20	Insulin R	IGF-I R	D23, D24	Eph R	EphA4
B21, B22	Axl	Axl	E1, E2	Eph R	EphA6
B23, B24	Axl	Dtk	E3, E4	Eph R	EphA7
C1, C2	Axl	Mer	E5, E6	Eph R	EphB1
C3, C4	HGF R	HGF R	E7, E8	Eph R	EphB2
C5, C6	HGF R	MSP R	E9, E10	Eph R	EphB4
C7, C8	PDGF R	PDGF Rα	E11, E12	Eph R	EphB6
C9, C10	PDGF R	PDGF Rβ	E13, E14	Insulin R	ALK
C11, C12	PDGF R	SCF R	E15, E16	___	DDR1
C13, C14	PDGF R	Flt-3	E17, E18	___	DDR2
C15, C16	PDGF R	M-CSF R	E19, E20	Eph R	EphA5
C17, C18	RET	c-Ret	E21, E22	Eph R	EphA10
C19, C20	ROR	ROR1	F1, F2	Reference Spots	___
C21, C22	ROR	ROR2	F5, F6	Eph R	EphB3
C23, C24	Tie	Tie-1	F7, F8	___	RYK
			F23, F24	Control(-)	PBS

Table 2: Phospho-RTK array coordinates.

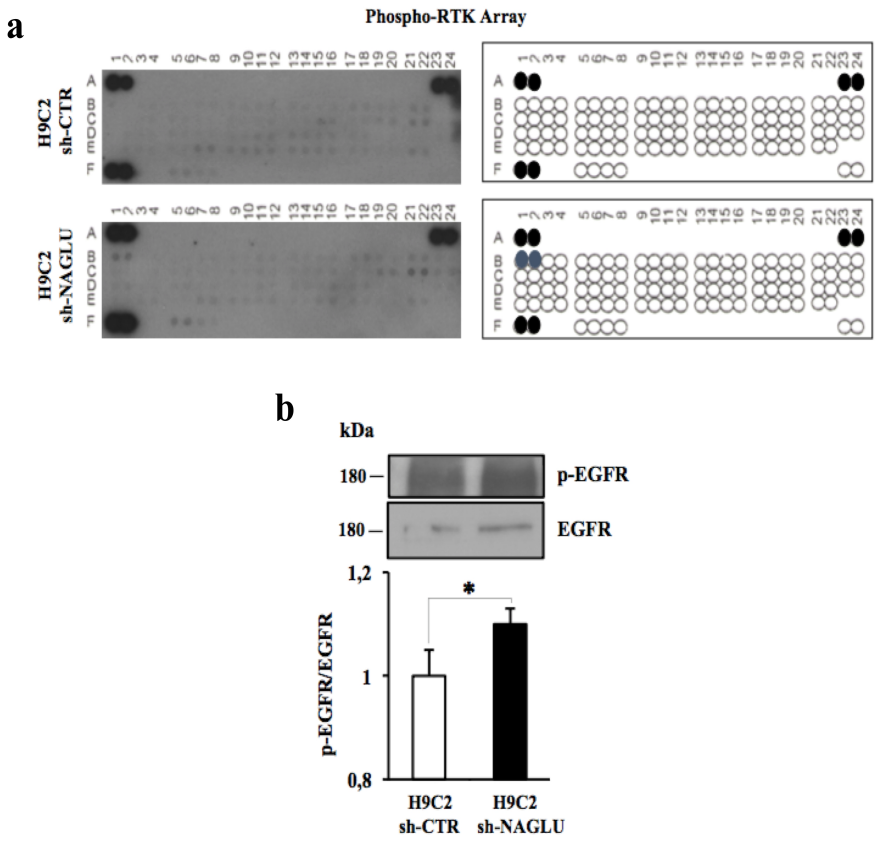

Figure 15: EGFR activation in NAGLU silenced H9C2 cardiomyoblasts. (a) p-RTK array showing the effect of NAGLU silencing on RTK phosphorylation. Cell lysates of H9C2 sh-CTR and H9C2 sh-NAGLU were applied (left panels) to p-RTK arrays. The chemiluminescent film images (right panels) are shown. The blue dots in the lower panels indicate the position of EGFR. **(b)** EGFR phosphorylation levels in H9C2 sh-NAGLU and H9C2 sh-CTR cells as measured by Western blotting analysis. To monitor protein loading, the upper blot was stripped and re-probed using anti-EGFR antibody. Densitometric analysis of the bands was performed and the data obtained are reported on the histogram below. *P<0.05

The involvement of EGFR activation in the hypertrophic response induced by NAGLU silencing in H9C2 cardiomyoblasts was confirmed by the observation that the treatment of H9C2sh-NAGLU with the specific EGFR inhibitor AG1478 (Levitzki A., et al., 1995) caused a signifcant reduction of ANP and BNP mRNA levels as compared to the untreated clones (Figure 16). No effect of AG1478 treatment was observed on ANP and BNP mRNA levels in H9C2 sh-CTR cells.

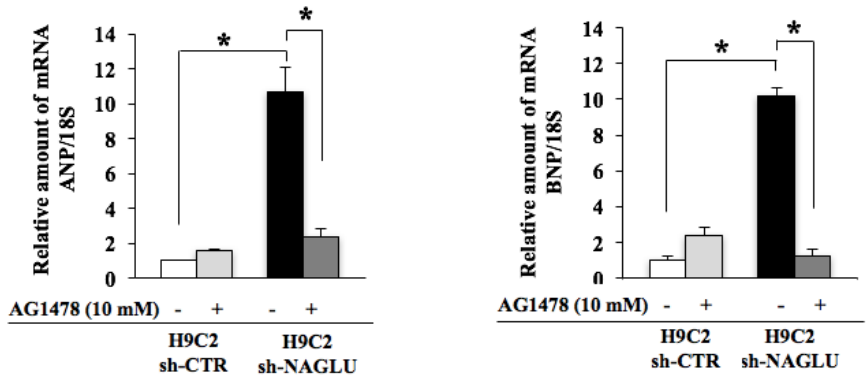

Figure 16: EGFR inhibition impairs the hypertrophic response in NAGLU silenced H9C2 cardiomyoblasts. Expression levels of mRNA coding for ANP and BNP both in the absence and presence of AG1478 in H9C2sh-NAGLU and H9C2sh-CTR as measured by quantitative RT-PCR analysis. The amount of ANP and BNP mRNA was normalized with respect to the amount of 18S ribosomal RNA housekeeping gene. *P<0.05

Furthermore, the AG1478 treatment did not affect the cell size of H9C2 sh-CTR as measured by phalloidin staining (Figure 17, upper panels), whereas a significant reduction of the cell dimensions of NALGU-depleted H9C2 upon AG1478 treatment was detected (Figure 17, lower panels). These results demonstrate that EGFR inhibition is able to rescue the hypertrophic phenotype of NALGUsilenced H9C2 cardiomyoblasts.

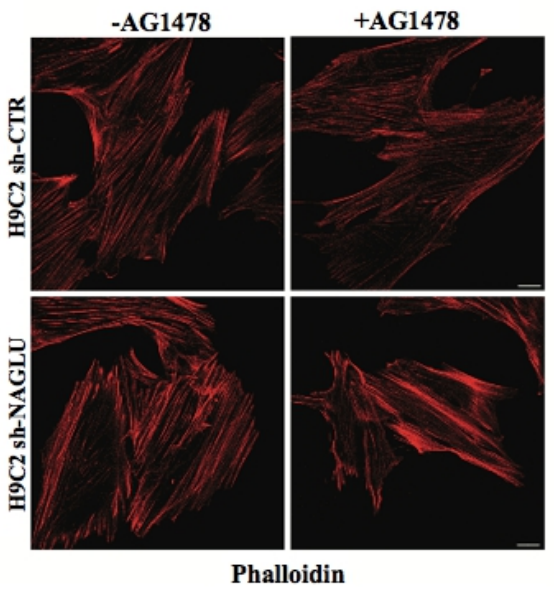

Figure 17: Abrogation of the hypertrophic phenotype by EGFR inhibition in NAGLU silenced H9C2 cardiomyoblasts. Representative images of actin cytoskeleton stained with phalloidin of H9C2 sh-CTR and H9C2 sh-NAGLU, both untreated and treated for 24 h with 10 μM of AG1478. Scale bars: 10 μm. A significant reduction of cell size was observed in AG1478 treated NAGLU-depleted H9C2 (lower panels), while no effect was detected in H9C2 sh-CTR clones (upper panels).

To establish the EGFR contribution to MPS IIIB lysosomal storage disorder in cardiac cells, we measured LAMP2 lysosomal-membrane associated protein levels in H9C2sh-NAGLU and control clones in the presence of the EGFR inhibitor AG1478. AG1478 treatment was able to significantly reduce LAMP2 protein expression levels in NAGLU-depleted cardiomyoblasts, whereas it did not influence LAMP2 protein levels in control clones (Figure 18a). Consistently, LysoTracker staining showed that H9C2sh-NAGLU treated with AG1478 have a reduced lysosome staining compared to untreated cells (Figure 18b).

These results definitely indicate that EGFR inhibition reduces both hypertrophy and lysosomal defects in NAGLU silenced H9C2 cardiomyoblasts.

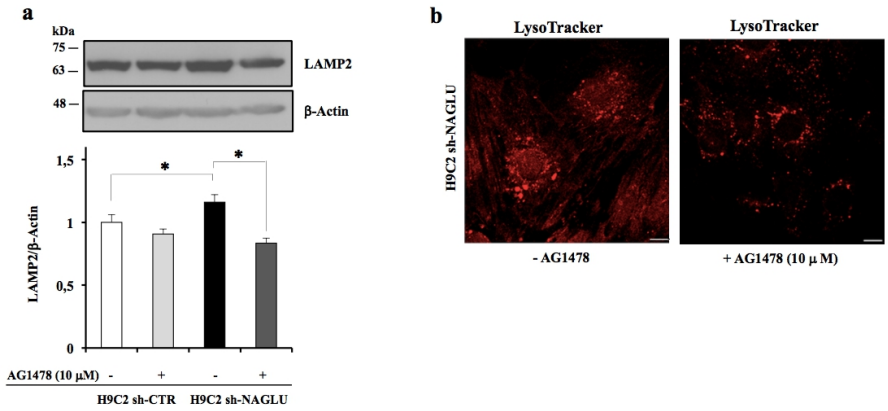

Figure 18: Reduction of lysosomal pathology by EGFR inhibition in NAGLU silenced H9C2 cardiomyoblasts. (a) LAMP2 protein expression levels both in absence and presence of AG1478 in H9C2sh-NAGLU and H9C2sh-CTR as measured by Western blotting analysis. The amount of LAMP2 as measured by densitometry was normalized with respect to the amount of β-actin. *P<0.05. **B.** Fluorescent staining of lysosomes in H9C2sh-NAGLU and H9C2sh-NAGLU treated with 10 μM of AG1478 labeled by LysoTracker probe. In the AG1478 treated clones, lysosome staining and cell size was reduced compared to the untreated clones.

4.4 EGFR activation triggers ERK1/2 phosphorylation in NAGLU-depleted H9C2 cardiomyoblasts.

The findings above reported prompted us to explore the EGFR signal transduction pathway contributing to the hypertrophic phenotype in NAGLU silenced cardiomyoblasts. Since previous evidence indicated that the phosphorylation of ERK1/2, a downstream target of EGFR, represents an essential regulator of the hypertrophic response (Bueno O.F. et al., 2002), we evaluated the phosphorylation levels of ERK1/2 in NAGLU-depleted rat cardiomyoblasts by Western blotting analysis. A significant increase in the phosphorylation levels of ERK1/2 in H9C2sh-NAGLU compared to control clones was observed (Figure 19a). Moreover, cell treatment with AG1478 resulted in a significant decrease of ERK1/2 phosphorylation in H9C2sh- NAGLU (Figure 19b), indicating that ERK1/2 activation in NAGLU-depleted cardyomyoblasts is likely EGFR-dependent.

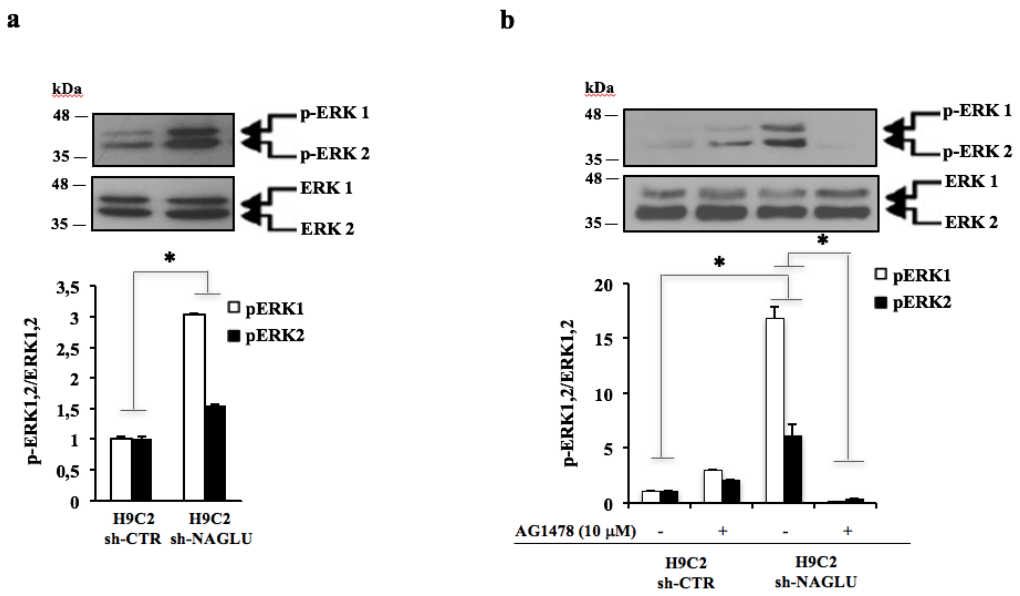

Figure 19: Enhanced ERK1/2 phosphorylation in NAGLU silenced H9C2 cardiomyoblasts. (a) ERK1/2 phosphorylation levels in H9C2sh-NAGLU and H9C2sh-CTR as measured by Western blotting. To monitor equal loading of protein in the gel lanes, the upper blot was stripped and re-probed using anti-ERK1/2 antibody. Densitometric analysis of the bands was performed and the data obtained are reported on the histogram below. *P<0.05. **(b)** ERK1/2 phosphorylation levels in H9C2sh-NAGLU and H9C2sh-CTR in the absence and in the presence of AG1478 as measured by Western blotting. To monitor protein loading of gel lanes, the upper blot was stripped and re-probed using anti anti-ERK1/2 antibody. Densitometric analysis was performed and the data obtained are reported on the histogram below. *P<0.05.

Then, we evaluated the effect of PD98059, a selective inhibitor of the MEK/ERK pathway (Ng D.C., et al., 2001; Pavone L.M., et al., 2011) on ERK1/2 phosphorylation in H9C2sh-NAGLU and H9C2sh-CTR. The treatment of H9C2sh-NAGLU with, PD98059 caused a drastic reduction of ANP mRNA levels (Figure 20a), thus suggesting that ERK1/2 phosphorylation is essential for the development of the hypertrophic phenotype. Furthermore, phalloidin staining of H9C2 sh-CTR and H9C2 sh-NAGLU exposed to PD98059 showed that the inhibitor treatment did not affect cell size of H9C2 sh-CTR (Figure 20b, upper panels), whereas

it caused a significant reduction of the cell dimensions in H9C2 sh-NAGLU compared to the untreated clones (Figure 20b, lower panels).

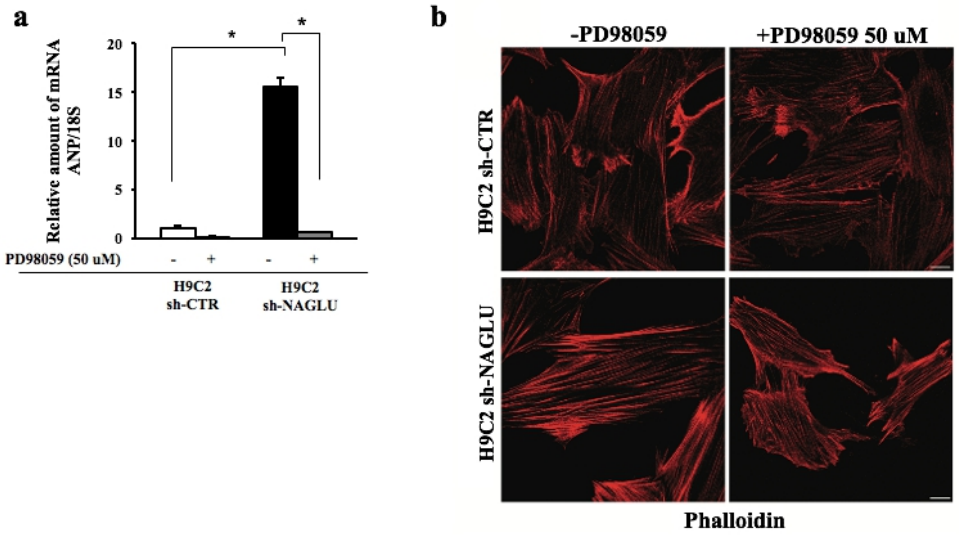

Figure 20: Reduction of cell size enlargement by MEK/ERK inhibition in NAGLU silenced H9C2 cardiomyoblasts. (a) Expression levels of mRNAs coding for ANP in H9C2sh-NAGLU and H9C2sh-CTR, in the absence and presence of PD98059, as measured by quantitative RT-PCR analysis. The amount of ANP mRNA was normalized with respect to the amount of 18S ribosomal RNA housekeeping gene. *P<0.05. **(b)** A significant reduction of cell size was observed in PD98059 treated NAGLU-depleted H9C2 (lower panels), while no effect was detected in H9C2 sh-CTR clones (upper panels).

4.5 NAGLU depletion in H9C2 cardiomyoblasts induces c-Src activation.

A direct link between EGFR signaling and enhanced Src-family kinase activity has been established (Biscardi J.S., et al., 1999). Therefore, we investigated the phosphorylation levels of c-Src in H9C2sh-NAGLU and control clones. A significant increase of c-Src phosphorylation was found in NAGLU-depleted H9C2 as compared to H9C2sh-CTR (Figure 21a). The treatment of H9C2sh-NAGLU with the EGFR inhibitor AG1478 did not reduce c-Src phosphorylation levels (Figure 21b), thus suggesting that c-Src phosphorylation represents an upstream event in EGFR activation following NAGLU depletion.

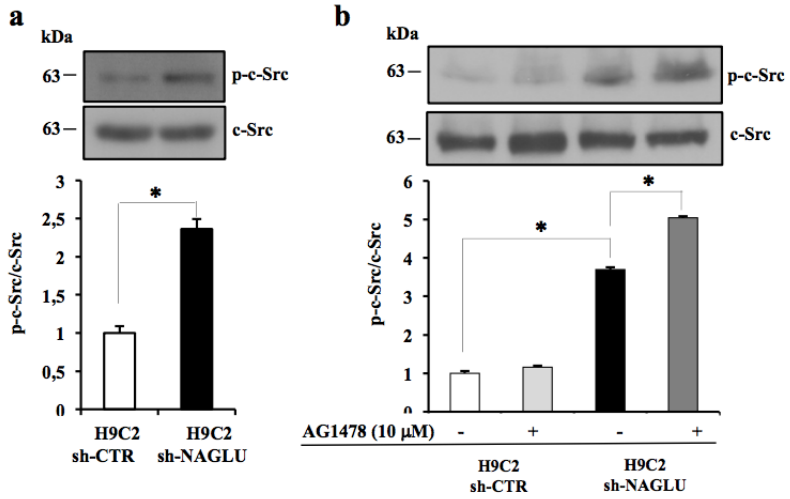

Figure 21: c-Src activation in NAGLU depleted H9C2 cardiomyoblasts. (a) c-Src phosphorylation levels in H9C2sh-NAGLU and H9C2sh-CTR as measured by Western blotting . To monitor protein loading of gel lanes, the upper blot was stripped and re-probed using anti-c-Src antibody. Densitometric analysis of the bands was performed and the data obtained are reported on the histogram below. *P<0.05. **(b)** c-Src phosphorylation levels in H9C2sh-NAGLU and H9C2sh-CTR, in the absence and presence of AG1478 as measured by Western blotting. To monitor protein loading, the upper blot was stripped and re-probed using anti-c-Src antibody. Densitometric analysis was performed and the data obtained are reported on the histogram below. *P<0.05.

Furthermore, Western blotting analysis showed that EGFR phosphorylation is reduced in the H9C2sh- NAGLU transfected with a dominant negative (DN) c-Src (Figure 22), indicating that EGFR phosphorylation in this MPS IIIB cellular model is mediated by c-Src.

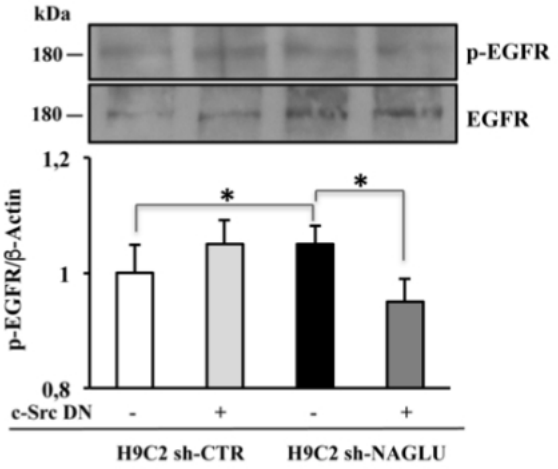

Figure 22: Reduction of EGFR phosphorylation by c-Src interfering in NAGLU depleted H9C2. EGFR phosphorylation levels in H9C2 sh-NAGLU and H9C2 sh-CTR cells transfected with DN c-Src as measured by Western blotting. The amount of EGFR phosphorylation as measured by densitometry was normalized with respect to the amount of ß-actin. *P<0.05.

Subsequently, the involvement of c-Src activation in the hypertrophic phenotype of NAGLU-depleted cardiomyoblasts was evaluated by measuring ANP mRNA levels in H9C2sh-NAGLU transfected with DN or wild-type (WT) c-Src. A significant reduction of ANP mRNA levels was observed in H9C2sh-NAGLU in the presence of DN c-Src (Figure 23a), whereas ANP mRNA levels strongly increased in the presence of WT c- Src (Figure 23b). By contrast, transfection with DN c-Src or WT c-Src had no effect on ANP mRNA levels in H9C2sh-CTR. Overall, these results suggest that c-Src activation contributes to the hypertrophic response in NAGLU-depleted cardiomyoblasts by activating EGFR signaling.

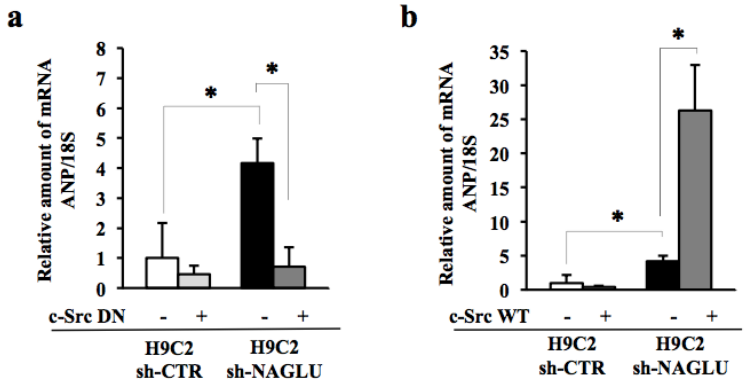

Figure 23: Reduction of the hypertrophic response by c-Src interfering causes in NAGLU depleted H9C2. (a) Expression levels of mRNAs coding for ANP in H9C2sh-NAGLU and H9C2sh-CTR transfected with DN c-Src as measured by quantitative RT-PCR analysis. The amount of ANP and BNP mRNA was normalized with respect to the amount of 18S ribosomal RNA housekeeping gene. *P<0.05. **(b)** Expression levels of mRNAs coding for ANP of in H9C2sh-NAGLU and H9C2sh-CTR transfected with WT c-Src, as measured by quantitative RT- PCR analysis. The amount of ANP and BNP mRNA was normalized with respect to the amount of 18S ribosomal RNA housekeeping gene. *P<0.05.

4.6 NAGLU depletion in H9C2 cardiomyoblasts results in increased expression levels of heparin-binding EGF-like growth factor (HB- EGF)

Multiple evidence demonstrated that the progressive accumulation of HS proteoglycans (HSPGs) on the cell membrane and extracellular matrix contributes to the pathogenesis of MPS diseases (Watson H.A. et al., 2014; Pan C. et al., 2005). The extracellular HSPGs can bind and regulate the activity of the EGFR ligand HB-EGF (Prince R.N. et al., 2010), and EGFR activation by HB-EGF plays a role in the hypertrophic signaling in cardiomyocytes (Yoshioka J., et al., 2005). Thus, we investigated by Western blotting analysis the expression levels of HB-EGF in in H9C2sh-NAGLU and control cells. A significant increase of the expression levels of HB-EGF protein was detected in H9C2sh-NAGLU as compared to control clones (Figure 24).

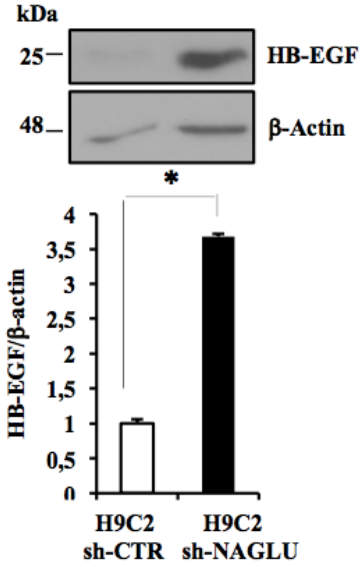

Figure 24: Up-regulation of heparin-binding EGF-like growth factor (HB-EGF) in NAGLU silenced H9C2 cardiomyoblasts. HB-EGF protein expression levels in H9C2sh-NAGLU and H9C2sh- CTR as measured by Western blotting. The amount of HB-EGF as measured by densitometry was normalized with respect to the amount of ß-actin. *P<0.05.

Furthermore, we investigated whether HB-EGF silencing by a specific siRNA result in the reduction of the EGFR induced hypertrophic response. Upon silencing of HB-EGF protein in H9C2sh-NAGLU (Figure 25a), we detected a reduction of ANP mRNA levels compared to the same cells treated with a scrambled siRNA (Figure 25b). These findings suggest that NAGLU-deficient cardiomyoblasts develop a hypertrophic phenotype through a coordinated intracellular and extracellular EGFR activation via c-Src and HB-EGF, respectively.

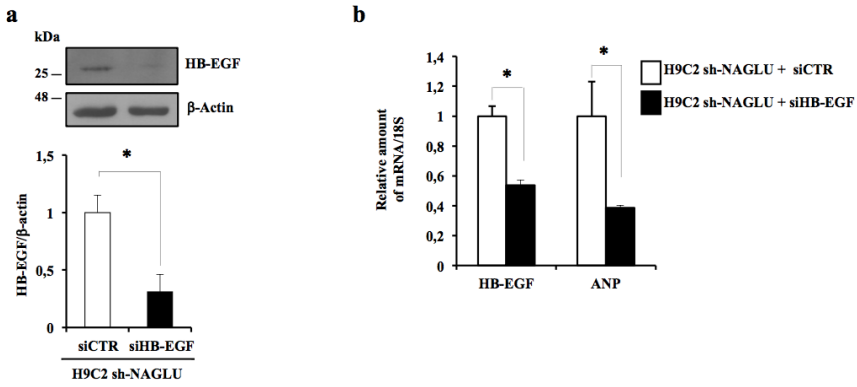

Figure 25: Reduction of the hypertrophic response by silencing of HB-EGF in NAGLU silenced H9C2 cardiomyoblasts. (a) Silencing of HB-EGF protein in H9C2sh-NAGLU and H9C2sh- CTR as measured by Western blotting. The amount of HB-EGF as measured by densitometry was normalized with respect to the amount of ß-actin. *P<0.05. **(b)** Expression levels of mRNAs coding for HB-EGF and ANP in H9C2sh-NAGLU transfected with HB-EGF siRNA and CTR siRNA as measured by quantitative RT- PCR analysis. The amount of HB-EGF and ANP mRNAs were normalized with respect to the amount of 18S ribosomal RNA housekeeping gene. *P<0.05.

5. DISCUSSION

In MPS IIIB disease, NAGLU deficiency leads to the accumulation of abnormal levels of HS in the lysosomes of the cells as well as in the extracellular matrix which accounts for a number of pathologic events affecting various tissues and organs, including brain, liver, spleen, kidney, and heart (Ballabio A., et al., 2009). Indeed, both during development and adult life, HS, which is a component of the cell surface and extracellular matrix-associated proteoglycans, plays crucial roles in the regulation of many physiological processes due to its property to bind and interact with signaling proteins, morphogens, growth factors, and other critical molecules (Iozzo R.V., et al. 2015; Pan C., et al., 2005; Bernfield M., et al., 1999; Kim S.H. et al., 2011). The extracellular accumulation of HS has been shown to impair fibroblast growth factor 2 (FGF-2) receptor binding and signaling in cells derived from MPS I patients (Pan C. et al., 2005). Here, we provide the first evidence that abnormal HS accumulation in a MPS IIIB cellular model is associated with the activation of EGFR signaling resulting in a hypertrophic phenotype.

The NAGLU-depleted cellular model generated by us fully represents the MPS IIIB lysosomal phenotype, showing lysosomal enlargement and cellular vacuolization. Furthermore, the increased levels of ANP and BNP mRNA in NAGLU-depleted cardiomyoblasts demonstrate that NAGLU silencing in H9C2 reproduces the hypertrophic phenotype previously detected in the cardiac tissues of NAGLU knock out mice (Schiattarella G.G., et al., 2015). Evidence exists about the involvement of EGFR in the onset of cardiac hypertrophy (Ai W. et al., 2010; Esposito G., et al., 2011). In this study, a phospho- RTK array showed the specific activation of EGFR in NAGLU-depleted cardiomyoblasts. Treatment of NAGLU-depleted H9C2 with the selective EGFR inhibitor AG1478 strongly reduced the levels of ANP and BNP mRNA. The inhibition of EGFR activation by AG1478 also resulted in the reduction of lysosomal defects in NAGLU-depleted cardiomyoblasts. These data suggest an active role of EGFR in the cellular events downstream HS accumulation, including those effects that lead to cardiac hypertrophy in MPS IIIB disease.

Although the pathogenesis of cardiac hypertrophy involves a number of complex molecular mechanisms (Heineke J., et al., 2006), the MEK1/ERK1/2 pathway plays a central role in the regulation of the cellular processes that lead to cardiac hypertrophy (Bueno O.F. et al., 2002). Moreover, the major actors of cardiac hypertrophy including ERKs and JNKs are activated by EGFR (Heineke J. et al., 2006; Duquesnes N.,

et al., 2009). Accordingly to the above evidence, in NAGLU-depleted cardiomyoblasts we found increased ERK1/2 phosphorylation, which was inhibited by the EGFR inhibitor AG1478. Furthermore, inhibition of ERK1/2 phosphorylation with the MEK/ERK inhibitor PD98059 strongly reduced ANP mRNA expression levels in NAGLU-depleted cardiomyoblasts. These results clearly demonstrate that the hypertrophic phenotype detected in the MPS IIIIB cellular model is associated with ERK1/2 phosphorylation promoted by EGFR activation.

Commonly, EGFR activation occurs either by binding with ligands such as EGF and HB-EGF, or by transactivation. Cellular Src (c-Src), a membrane-associated tyrosine kinase, is required for many EGFR-mediated cellular functions (Biscardi J.S. et al., 1999, Luttrell L.M., et al., 1997; Wu W.J., et al., 2003). The interactions between EGFR and c-Src are bi-directional, and their consequence is an enhanced phosphorylation of specific substrates. In this study, we found increased c-Src phosphorylation levels in NAGLU- depleted cardiomyoblasts compared control cells, and c-Src phosphorylation resulted to be unaffected by treatment with AG1478. Furthermore, our investigations showed that both EGFR phospshorylation and ANP mRNA expression levels are respectively down-regulated or up-regulated by transfecting H9C2sh-NAGLU cardiomyoblasts with DN or WT c-Src. These findings indicate that in NAGLU-depleted cardiomyoblasts c-Src phosphorylation mediates EGFR activation with subsequent signaling leading to the hypertrophic phenotype.

Together with the activation of EGFR by c-Src, we also found in our cellular model the up-regulation of the EGFR ligand HB- EGF. The progressive accumulation of HSPGs on the cell membrane and extracellular matrix contributes to the pathogenesis of MPS diseases (Watson H.A, et al. 2014; Pan C., et al., 2005; Ballabio A. et al., 2009). Extracellular HSPGs may sequester soluble secreted growth factors and facilitate their binding to the cognate receptors, thus activating receptor signaling (Iozzo R.V. et al., 2015; Bernfield M. et al. 1999; Faye C., et al., 2009). Moreover, HSPGs may also interact with growth factors anchored to the cell surface via a trans-membrane domain, and especially those belonging to the EGFR-ligand family, which include HB-EGF (Prince R.N., et al., 2010). The proteolytic cleavage of the anchored form of HB-EGF, proHB-EGF, at the extracellular domain gives rise to the soluble form of HB-EGF. It has been demonstrated that HB-EGF plays an important role in cardiac heart development (Iwamoto R., et al., 2010), and hypertrophy (Yoshioka J., et al., 2005; Lee K.S., et al., 2011). Angiotensin II-mediated transactivation of EGFR appears to involve Src-

mediated MMP-activated release of HB-EGF (Eguchi S., et al., 2001). Transactivation of RTKs by G protein-coupled receptors (GPCRs) is a common pathway for transmission of reactive oxygen species (ROS)-sensitive signals, and interaction between GPCRs and RTKs may occur either in a ligand- independent manner involving membrane associated non-receptor tyrosine kinases, such as c-Src, or through the activation of metalloproteases (MMPs) which induce the release of RTK ligands (Little P.J., et al., 2013; Cattaneo F., et al., 2014) such as HB-EGF. Indeed, the increased HB-EGF expression levels and the reduction of the hypertrophic response following HB-EGF silencing observed in NAGLU-depleted cardiomyoblasts suggest that in the MPS IIIB cellular model HB-EGF plays a part in EGFR activation and subsequent signaling leading to hypertrophy. Based on our findings and the literature we unraveled the signaling mechanism by which NAGLU silencing, lysosomal defects and the excess of extracellular HSPGs promote hypertrophy through c-Src and HB-EGF-mediated activation of EGFR linking to ERK1/2 pathway.

6. CONCLUSION AND PERSPECTIVES

Until recently, no effective approved therapy for MPS IIIB is available. Substrate reduction therapy based on the use of small molecules with inhibitory activity of GAG synthesis has been tested as a possible treatment for MPS diseases. In particular, genistein, a compound belonging to the family of isoflavones, was shown to decrease GAG synthesis in fibroblasts from MPS I, II, IIIA and IIIB (Piotrowska E., et al., 2006). Indeed, genistein is able to inhibit the kinase activity of EGFR required for the regulation of the activity of particular transcription factors involved in GAG synthesis (Moskot M., et al., 2014). However, genistein only partially ameliorates the clinical symptoms of MPS III patients (De Ruijter J., et al., 2012). Our findings highlight the central role of EGFR activation in the hypertrophic phenotype and lysosomal pathology related to cardiac disease in MPS IIIB. In particular, our study demonstrates that NAGLU deficiency, leading to abnormal accumulation of either intracellular or extracellular HS, triggers c-Src activation and HB-EGF up-regulation, both promoting EGFR signaling activation. The EGFR downstream activation of RK signaling cascade finally results in hypertrophy.

In conclusion, the results of our study not only contribute to a better understanding of the molecular mechanisms underlying cardiac disease in MPS IIIB, but also provide novel clues for EGFR pathway targeting-based approaches for MPS IIIB as well as for other MPS diseases.

7. ACKNOWLEDGEMENTS

Three years ago, when I started my PhD, I was really confident and determined to start a good route for the realization of my research project. Despite my dedication, there was a moment where I missed this confidence since I realized that this job can show you a lot of difficulties, and you should be emotionally strong to overcome them. Although this feeling, I found the motivation to carry on and after three years I really would like to continue this career because I still love science. I guess that it is one of the main goal at the end of your PhD career.

First of all, I would like to express my gratitude to my ***Professor Luigi Michele Pavone****, who has supervised me all the time, for his motivation, encouragements and his guidance in these three years. I also aknowledge him for appreciating my scientific proposal and letting me free to follow my ideas, while guiding me with valuable advice. Thanks*

for giving me the opportunity to grow professionally working abroad and gain more scientific independence.
Thank you for your patience *and the time spent with me in working together before deadlines, despite your busy days.*
Thank you for your confidence and trust on me.

I would like to aknowledge ***Dr. Valeria De Pasquale*** *for her technical and scientific help. Thank you for your determination and the hard work in the realization of H9C2 stable clones that persecuted us for two years.*

I could never forget the thousands of Western Blotting that we did together with never giving up and the happiness of a good result! Thanks for teaching me how to work with accuracy and precision, for our complicity and for all the fun that we have had during these years.

My sincere aknowledgements are also extended to all the people that I met during my PhD course, with special thanks to ***Dr. Francesca Cammarota*** *who shared with me this experience. Thank you for to be always a kindly and lovable person in all the circumstances, and for the nice interaction every day. Thanks for your support during my period abroad and for the long conversations by phone keeping me company in the hard moments.*

For the goal achieved with this research project I also would like to thank all the people that gave their contribution to it. Thanks to ***Professor Vittorio Enrico Avvedimento*** *and* ***Dr. Antonio Pezone*** *who shared with us their knowledge and for their kind collaboration.*

My gratitude extends to ***Professor Norma Staiano*** *for her constant commitment to reviewing this manuscript.*

In the end, a final thought goes to my family for their love and affection, for supporting me along the way, and for their moral support in my life in general.

8. REFERENCES

Ai W., Zhang Y., Tang Q.Z., Yan L., Bian Z.Y., Liu C., Huang H., Bai X., Yin L., Li H. (2010). Silibinin attenuates cardiac hypertrophy and fibrosis through blocking EGFR-dependent signaling. J Cell Biochem 110, 1111-1122

Ballabio A. (2009). Disease pathogenesis explained by basic science: lysosomal storage diseases as autophagocytic disorders. Int J Clin Pharmacol Ther 47, S34-S38

Ballabio A., Gieselmann V. (2009). Lysosomal disorders: From storage to cellular cellular damage. Biochim Biophys Acta 1793, 684-696

Bax M.C., Colville G.A. (1995). Behaviour in mucopolysaccharide disorders. Arch Dis Child 73, 77-81

Bernfield M., Gotte M., Park P.W., Reizes O., Fitzgerald M.L., Lincecum J., Zako M. (1999). Functions of cell surface heparan sulfate proteoglycans. Annu Rev Biochem 68, 729–777

Biscardi J.S., Maa M.C., Tice D.A., Cox M.E., Leu T.H., Parsons S.J. (1999). c-Src-mediated phosphorylation of the epidermal growth factor receptor on Tyr845 and Tyr1101 is associated with modulation of receptor function. J Biol Chem 274, 8335-8343

Bovolenta P., Fernaud-Espinosa I. (2000). Nervous system proteoglycans as modulators of neurite growth. Prog Neurobiol 61,113-132

Braulin E.A., Harmatz P.R., Scarpa M., Furlanetto B., Kampmann C., Loehr J.P., ponder K.P., Roberts W.C., Rosenfeld H.M., Giugliani R., (2011). Cardiac disease in patients with mucopolysaccharidosis: presentation, diagnosis and management. J Inherit Metab Dis 34, 1183–1197

Bueno O.F., Molkentin J.D. (2002). Involvement of extracellular signal-regulated kinases 1/2 in cardiac hypertrophy and cell death. Circ Res 91, 776–781

Cardone L., Carlucci A., Affaitati A., Livigni A., De Cristofaro T., Garbi C. *et al.* (2004). Mitochondrial AKAP121 binds and targets protein tyrosine phosphatase D1, a novel positive regulator of src signaling. Mol Cell Biol 24, 4613-4626

Carlsson S.R., Fukuda M. (1990). The polylactosaminoglycans of human lysosomal membrane glycoproteins lamp-1 and lamp-2. Localization on the peptide backbones. J Biol Chem 265, 20488–20495

Cattaneo F., Guerra G., Parisi M., De Marinis M., Tafuri D., Cinelli M., Ammendola R. (2014). Cell-surface receptors transactivation mediated by g protein-coupled receptors. Int J Mol Sci 15, 19700-19728

Chapman H. A. (1998). Endosomal proteolysis and MHC class II function. Curr Opin Immunol 10, 93-102

Chazotte B. Labeling membranes with fluorescent phosphatidylethanolamine. Cold Spring Harb Protoc 2011; 2011

Cleary M . A . , Wraith J.E. (1993). Management of mucopolysaccharidosis type III. Arch Dis Child. 69, 403-406

Conus S., Perozzo R., Reinheckel T., Peters C., Scapozza L., Yousefi S. and Simon H. U. (2008). Caspase-8 is activated by cathepsin D initiating neutrophil apoptosis during the resolution of inflammation. J Exp Med 205, 685-98

de Ruijter J., Valstar M.J., Narajczyk M., Wegrzyn G., Kulik W., Ijlst L., Wagemans T., van der Wal W.M., Wijburg F.A. (2012). Genistein in Sanfilippo disease: a randomized controlled crossover trial. Ann Neurol 71, 110-120

Di Domenico C., Villani G.R., Di Napoli D., Nusco E., Calì G., Nitsch L., Di Natale P. (2009). Intracranial gene delivery of LV-NAGLU vector corrects neuropathology in murine MPS IIIB. Am J Med Genet A. 2, 639-646

Di Natale P., Di Domenico C., Gargiulo N., Castaldo S., Gonzalez Y. Reyero E., Mithbaokar P., De Felice M., Follenzi A., Naldini L., Villani G.R. (2005). Treatment of the mouse model of mucopolysaccharidosis type IIIB with lentiviral-NAGLU vector. Biochem J 388, 639-646

Di Natale P., Salvatore D., Daniele A., Bonatti S. (1985) Biosynthesis of ! ! N-acetylglucosaminidase in cultured human kidney carcinoma cells. Enzyme 33, 75-83

Driessen C., Bryant R. A., Lennon-Dumenil A. M., Villadangos J. A., Bryant P. W., Shi G. P., Chapman H. A. and Ploegh H. L. (1999). Cathepsin S controls the trafficking and maturation of MHC class II molecules in dendritic cells. J Cell Biol 147, 775-90

Duquesnes N., Vincent F., Morel E., Lezoualc'h F., Crozatier B. (2009). The EGF receptor activates ERK but not JNK Ras-dependently in basal conditions but ERK and JNK activation pathways are predominantly Ras-independent during cardiomyocyte stretch. Int J Biochem Cell Biol 41, 1173-1181

Eguchi S., Dempsey P.J., Frank G.D., Motley E.D., Inagami T. (2001). Activation of MAPKs by angiotensin II in vascular smooth muscle cells. Metalloprotease-dependent EGF receptor activation is required for activation of ERK and p38 MAPK but not for JNK. J Biol Chem 276, 7957-7962

Ellinwood N.M., Wang P., Skeen T., Sharp N.J., Cesta M., Decker S., Edwards N.J., Bublot I., Thompson J.N., Bush W., Hardam E., Haskins M.E., Giger U. (2003). A model of mucopolysaccharidosis IIIB (Sanfilippo syndrome type IIIB): N-acetyl-alpha-D-glucosaminidase deficiency in Schipperke dogs. J Inherit Metab Dis 26, 489-504

Esko J.D., Selleck S.B. (2002). Order out of chas: Assembly of ligand binding sites in heparan sulfate. Annu Ver Biochem 71, 435-471

Esposito G., Perrino C., Cannavo A., Schiattarella G.G., Borgia F., Sannino A., Pironti G., Gargiulo G., Di Serafino L., Franzone A., Scudiero L., Grieco P., Indolfi C., Chiariello M. (2011). EGFR trans-activation by urotensin II receptor is mediated by β-arrestin recruitment and confers cardioprotection in pressure overload-induced cardiac hypertrophy. Basic Res Cardiol 106, 577-589

Faye C., Moreau C., Chautard E., Jetne R., Fukai N., Ruggiero F., Humphries M.J., Olsen B.R., Ricard-Blum S. (2009). Molecular interplay between endostatin, integrins, and heparan sulfate. J Biol Chem 284, 22029-22040

Freeman C., Parish C.R. (1998). Human platelet heparanase: purificaton, characterization and catalytic activity. Biochem J 330, 1341-1350

Fuller M., Chau A., Nowak C.R., Hopwood J.J., Meikle P.J. (2005). A defect in exodegradative pathways provides insight into endodegradation of heparan and dermatan sulfates. Glycobiology 16, 318-325

Gingis-Velitski S., Zetser A., Kaplan V., Bem-Zaken O., Cohen E., Levy-Adam F., et al. (2004). Heparanase uptake is mediated by cell membrane heparan sulfate protoglycans. J Biol Chem 279, 44084-44092

Hamano K., Hayashi M., Shioda K., Fukatsu R., Mizutani S. (2008). Mechanisms of neurodegeneration in mucopolysaccharidoses II and IIIB: analysis of human brain tissue. Acta Neuropathol 115(5):547-59 Heineke J., Molkentin J.D. (2006). Regulation of cardiac hypertrophy by intracellular signalling pathways. Nat Rev Mol Cell Biol 7, 589-600

Heineke J., Molkentin J.D. (2006). Regulation of cardiac hypertrophy by intracellular signalling pathways. Nat Rev Mol Cell Biol 7, 589-600

Heldermon C.D.1, Hennig A.K., Ohlemiller K.K., Ogilvie J.M., Herzog E.D., Breidenbach A., Vogler C., Wozniak D.F., Sands M.S. (2007). Development of sensory, motor and behavioral deficits in the murine model of Sanfilippo syndrome type B. PLoS One 2, e772

Heldermon C.D., Ohlemiller K.K., Herzog E.D., Vogler C., Qin E., Wozniak D.F., Tan Y., Orrock J.L., Sands M.S. (2010). Therapeutic efficacy of bone marrow transplant, intracranial AAV-mediated gene therapy, or both in the mouse model of MPS IIIB. Mol Ther 18, 873-880

Hoozemans J.J., van Haastert E.S., Nijholt D.A., Rozemuller A.J., Eikelenboom P., Scheper W. (2009). The unfolded protein response is activated in pretangle neurons in Alzheimer's disease hippocampus. Am J Pathol 174, 1241-1251

Hu H., Marton T.F., Goodman C.S. (2001). Plexin b mediates axon guidance in Drosophila by simultaneously inhibiting active rac and enhancing rhoa signaling. Neuron 32, 39-51

Iozzo R.V., Schaefer L. (2015). Proteoglycan form and function: a comprehensive nomenclature of proteoglycans. Matrix Biol 42, 11-55

Iwamoto R., Mine N., Kawaguchi T., Minami S., Saeki K., Mekada E. (2010). HB-EGF function in cardiac valve development requires interaction with heparan sulfate proteoglycans. Development 137, 2205-2214

Jellinger K.A. (2009). Recent advances in our understanding of neurodegeneration. J Neural Transm. 116, 1111-1162.

Karagiannis T.C., Lin A.J.E., Ververis K., Chang L., Tang M.M., Okabe J., El-Osta A. (2010). Trichostatin A accentuates doxorubicin-induced hypertrophy in cardiac myocytes Aging 2, 659–668

Kim S.H., Turnbull J., Guimond S. (2011). Extracellular matrix and cell signalling: the dynamic cooperation of integrin, proteoglycan and growth factor receptor. J Endocrinol 209, 139-151

Kjellén L., Lindahl U. (1991). Proteoglycans: structures and interactions. Annu Ver Biochem 60, 443-475

Lee K.S., Park J.H., Lim H.J., Park H.Y. (2011). HB-EGF induces cardiomyocyte hypertrophy via an ERK5-MEF2A-COX2 signaling pathway. Cell Signal 23, 1100-1109

Lemonnier T., Blanchard S., Toli D., Roy E., Bigou S., Froissart R., Rouvet I., Vitry S., Heard J.M., Bohl D. (2011). Modeling neuronal defects associated with a lysosomal disorder using patient- derived induced pluripotent stem cells. Hum Mol Genet 20, 3653-3666

Levitzki A., Gazit A. (1995). Tyrosine kinase inhibition: an approach to drug development. Science 267, 1782-1788

Li H.H., Yu W.H., Rozengurt N., Zhao H.Z., Lyons K.M., Anagnostaras S., Fanselow M.S., Suzuki K., Vanier M.T., Neufeld E.F. (1999). Mouse model of Sanfilippo syndrome type B produced by targeted disruption of the gene encoding alpha-N-acetylglucosaminidase. Proc Natl Acad Sci. 96, 14505-14510

Lin L., Rao Y., Isacson O. (2005). Netrin and Slit2 regulate and direct neurite growth of ventral midbrain dopaminergic neurons. Mol Cell Neurosci 28, 547-555

Little P.J. (2013). GPCR responses in vascular smooth muscle can occur predominantly through dual transactivation of kinase receptors and not classical Gαq protein signalling pathways. Life Sci 92, 951-956

Livak K.J., Schmittgen T.D. (2001) Analysis of relative gene expression data using real-time quantitative PCR and the 2(-Delta Delta C(T)) Method. Methods 25, 402-408.

Lopes C.C, Dietrich C.P., Nader H.B. (2006). Specific structural features of syndecans and heparan sulfate chains are needed for cell signaling. Braz J Med Biol Res 39, 157-167

Luttrell L.M., Della Rocca G.J., van Biesen T., Luttrell D.K., Lefkowitz R.J. (1997). Gbetagamma subunits mediate Src-dependent phosphorylation of the epidermal growth factor receptor. A scaffold for G protein-coupled receptor-mediated Ras activation. J Biol Chem 272, 4637-4644

Mikami T., Kitagawa H. (2013). Biosynthesis and function of chondroitin sulfate. Biochim Biophys Acta 1830, 4719-4733

Murrey H., Hsieh-Wilson L.C. (2008). The chemical neurobiology of carboydrates. Chem Ver 198, 1708-1731

Ma X., Tittiger M., Knutsen R.H., Kovacs A., Schaller L., Mecham R.P., Ponder K.P. (2008). Upregulation of elastase proteins results in aortic dilatation in mucopolysaccharidosis I mice. Mol Genet Metab 94, 298-304

Metcalf J.A., Linders B., Wu S Bigg P., O'Donnell P., Sleeper M.M., Whyte M.P., Haskins M., Ponder K.P. (2010). Upregulation of elastase activity in aorta in mucopolysaccharidosis I and VII dogs may be due to increased cytokine expression. Mol Genet Metab 99, 396–407

Meikle P.J., Ranieri E., Ravenscroft E.M., Hua C.T., Brooks D.A., Hopwood J.J. (1999). Newborn screening for lysosomal storage disorders. Southeast Asian J Trop Med Public Health. 2, 104-110

Malinowska M., Wilkinson F.L., Langford-Smith K.J., Langford-Smith A., Brown J.R., Crawford B.E., Vanier M.T., Grynkiewicz G., Wynn R.F., Wraith J.E., Wegrzyn G., Bigger B.W. (2010). Genistein improves neuropathology and corrects behaviour in a mouse model of neurodegenerative metabolic disease. PloS One 5, e14192

Ménard C., Pupier S., Mornet D., Kitzmann M., Nargeot J., Lory, P. (1999). Modulation of L-type calcium channel expression during retinoic acid-induced differentiation of H9C2 cardiac cells. J Biol Chem 274, 29063-29070

Moskot M., Montefusco S., Jakóbkiewicz-Banecka J, Mozolewski P., Węgrzyn A., Di Bernardo D., Węgrzyn G., Medina D.L., Ballabio A., Gabig-Cimińska M. (2014). The phytoestrogen genistein modulates lysosomal metabolism and transcription factor EB (TFEB) activation. J Biol Chem 289, 17054-17069

Neufeld E.F., Muenzer J. (2001) The mucopolysaccharidoses. In: Scriver CR, Beaudet AL, Sly WS, Valle D, editors. The metabolic and molecular bases of inherited disease, 8th Ed, McGraw-Hill, New York, pp. 3421–3452

Ng D.C., Long C.S., Bogoyevitch M.A. (2001). A role for the extracellular signal-regulated kinase and p38 mitogen-activated protein kinases in interleukin-1 beta-stimulated delayed signal tranducer and activator of transcription 3 activation, atrial natriuretic factor expression, and cardiac myocyte morphology. J Biol Chem 276, 29490-29498

Pan C. Nelson M.S., Reyes M., Koodie L., Brazil J.J., Stephenson E.J., Zhao R.C., Peters C., Selleck S.B., Stringer S.E., Gupta P. (2005). Functional abnormalities of heparan sulfate in mucopolysaccharidosis-I are associated with defective biologic activity of FGF-2 on human multipotent progenitor cells. Blood 106, 1956-1964

Parish C. R., Freeman C. (2001). Heparanase: a key enzyme involved in cell invasion. Biochem Biophys Acta 1471, M99-108

Pavone L.M., Cattaneo F., Rea S., De Pasquale V., Spina A., Sauchelli E., Mastellone V., Ammendola R. (2011). Intracellular signaling cascades triggered by the NK1 fragment of hepatocyte growth factor in human prostate epithelial cell line PNT1A. Cell Signal. 23, 1961-1971

Peng K., Tian X., Qian Y., Skibba M., Zou C., Liu Z., Wang J., Xu Z., Li X., Liang G. (2016). Novel EGFR inhibitors attenuate cardiac hypertrophy induced by angiotensin II. J Cell Mol Med 20, 482-494

Pereira V.G., Martins A.M., Micheletti C., D'Almeida V. (2008). Mutational and oxidative stress analysis in patients with mucopolysaccharidosis type I undergoing enzyme replacement therapy. Clin Chim Acta 387, 75-79

Piotrowska E., Jakóbkiewicz-Banecka J., Barańska S., Tylki-Szymańska A., Czartoryska B., Wegrzyn A., Wegrzyn G. (2006). Genistein-mediated inhibition of glycosaminoglycan synthesis as a basis for gene expression-targeted isoflavone therapy for mucopolysaccharidoses. Eur J Hum Genet 14, 846-852

Platt FM, Walkley SU. (2004). Lysosomal defects and storage. In Lysosomal Disorders of the Brain. Oxford University Press, Oxford. 32–49

Prince R.N., Schreiter E.R., Zou P., Wiley H.S., Ting A.Y., Lee R.T., Lauffenburger D.A. (2010). The heparin-binding domain of HB-EGF mediates localization to sites of cell-cell contact and prevents HB-EGF proteolytic release. J Cell Sci 123, 2308–2318

Reddy A., Caler E.V., Andrews N.W. (2001). Plasma membrane repair is mediated by Ca(2+)-regulated exocytosis of lysosomes. Cell 106, 157-169

Reolon G.K., Reinke A., de Oliveira M.R., Braga L.M., Camassola M., Andrades M.E., Moreira J.C., Nardi N.B., Roesler R., Dal-Pizzol F. (2009). Alterations in oxidative markers in the cerebellum and peripheral organs in MPS I mice. Cell Mol Neurobiol29, 443-448

Rigante D., Segni, G. (2002). Cardiac structural involvement in mucopolysaccharidoses. Cardiology 98, 18–20

Rodriguez A., Webster P., Ortego J. and Andrews N. W. (1997). Lysosomes behave as Ca2+-regulated exocytic vesicles in fibroblasts and epithelial cells. J Cell Biol 137, 93-104

Sarrazin S., Lamanna W.C., Esko J.D. (2011). Heparan sulfate proteoglycans. Cold Spring Harb Perspect Biol 3, pii: a004952

Salvatore D., Bonatti S., Di Natale P. (1984). Lysosomal α-N-acetylglucosaminidase: purification and characterisation of the human enzyme. Bull Mol Bio Med 9, 111-121

Sasaki T., Sukegawa K., Masue M., F ukuda S., Tomatsu S., Orii T. (1991). Purification and partial characterisation of α-N-acetylglucosaminidase from human liver. Biochem J 110, 842-846

Schiattarella G.G., Cerulo G., De Pasquale V., Cocchiaro P., Paciello O., Avallone L., Belfiore M.P., Iacobellis F., Di Napoli D., Magliulo F., Perrino C., Trimarco B., Esposito G., Di Natale P., Pavone L.M. (2015). The murine model of mucopolisaccharidosis IIIB develops cardiopathies over time leading to heart failure. PloS One 10, e 0131662

Schiattarella G.G., Hill J.A. (2016). Therapeutic targeting of autophagy in cardiovascular disease. J Mol Cell Cardiol. 95, 86-93 \l

Schiattarella G.G., Hill J.A. (2015). Inhibition of hypertrophy is a good therapeutic strategy in \lentricular pressure overload. Circulation 131, 1435-1447

Settembre C., Fraldi A., Jahreiss L., Spampanato C., Venturi C., Medina D., de Pablo R., Tacchetti C., Rubinsztein D.C. and Ballabio A. (2008). A block of autophagy in lysosomal storage disorders. Hum Mol Genet 17, 119-129

Simonaro C.M., Haskins M.E., Schuchman E.H. (2001). Articular chondrocytes from animals with a dermatan sulfate storage disease undergo a high rate of apoptosis and release nitric oxide and inflammatory cytokines: a possible mechanism underlying degenerative joint disease in the mucopolysaccharidoses. Lab Invest 81,319-328

Simonaro C.M., D'Angelo M., Haskins M.E., Schuchman E.H. (2005). Joint and bone disease in mucopolysaccharidoses VI and VII: identification of new therapeutic targets and biomarkers using animal models. Pediatr Res, 57, 701-707

Simonaro C.M., D'Angelo M., He X., Eliyahu E., Shtraizent N., Haskins M.E., Schuchman E.H. (2008). Mechanism of glycosaminoglycan-mediated bone and joint disease: implications for the mucopolysaccharidoses and other connective tissue diseases. Am Pathol 172, 112-122

Simonaro C.M., Ge Y., Eliyahu E., He X., Jepsen K.J., Schuchman E.H. (2010). Involvement of the Toll-like receptor 4 pathway and use of TNF-alpha antagonists for treatment of the mucopolysaccharidoses. Proc Natl Acad Sci USA 107, 222-227

Vitry S., Ausseil J., Hocquemiller M., Bigou S., Dos Santos Coura R., Heard J.M. (2009). Enhanced degradation of synaptophysin by the proteasome in mucopolysaccharidosis type IIIB. Mol Cell Neurosci 41,8-18

Vitry S., Bruyère J., Hocquemiller M., Bigou S., Ausseil J., Colle M.A., Prévost M.C., Heard J.M. (2010). Storage vesicles in neurons are related to Golgi complex alterations in mucopolysaccharidosis IIIB. Am J Pathol 177, 2984-2999

Von Figura K., Hasilik A., Steckel F., Van de Kamp J.J. (1984). Biosynthesis and maturation of alpha- N-acetylglucosaminidase in normal and Sanfilippo B fibroblast. Am J Hum Genet 36, 93-100

Walkley S.U., Vanier MT. (2009). Secondary lipid accumulation in lysosomal disease. Biochim Biophys Acta 1793, 726–736

Watkins S.J., Borthwick G.M., Arthur H.M. (2011). The H9C2 cell line and primary neonatal cardiomyocyte cells show similar hypertrophic responses in vitro. In Vitro Cell Dev Biol Anim 47, 125–131

Watson H.A., Holley R.J., Langford-Smith K.J., Wilkinson F.L., van Kuppevelt T.H., Wynn R.F., Wraith J.E., Merry C.L., Bigger B.W. (2014). Heparan sulfate inhibits hematopoietic stem and progenitor cell migration and engraftment in mucopolysaccharidosis I. J Biol Chem 289, 36194- 36203

Weber B., Blanch L., Clements P.R., Scott H.S., Hopwood J.J. (1996). Cloning and expression of the gene involved in Sanfilippo B syndrome (mucopolysaccharidosis III B Hum Mol Genet 5, 771–777

Weinstein I.B. (2000). Disorders in cell circuitry during multistage carcinogenesis: the role of homeostasis. Carcinogenesis 21, 857-864

Wei S.J., Williams J.G., Dang H., Darden T.A., Betz B.L., Humble M.M., Chang F.M., Trempus C.S. et al. (2008) Identification of a specific motif of the DSS1 protein required for proteasome interaction and p53 protein degradation. J Mol Biol 383, 693-712

Whitelock J.M., Iozzo R.V. (2005). Heparan sulfate: a complex polymer charged with biological activity. Chem Ver 105, 2745-2764

Wu W.J., Wang J., Cerione RA. (2003). Epidermal growth factor-dependent regulation of Cdc42 is mediated by the Src tyrosine kinase. J Biol Chem 278, 49293-49300

Yogalingam G., Weber B., Meehan J., Rogers J., Hopwood J.J. (2000). Mucopolysaccharidosis type IIIB: characterisation and expression of wild-type and mutant recombinant alpha-N-acetylglucosaminidase and relationship with sanfilippo phenotype in an attenuated patient. Biochim Biophys Acta 1502, 415-425.

Yoshioka J., Prince R.N., Huang H., Perkins S.B., Cruz F.U., MacGillivray C., Lauffenburger D.A., Lee R.T. (2005). Cardiomyocyte hypertrophy and degradation of connexin43 through spatially restricted autocrine/paracrine heparin-binding EGF. Proc Natl Acad Sci. USA 102, 10622-10627

Yu W.H., Woessner J.F., McNeish J.D., Stamenkovic I. (2002). CD44 anchors the assembly of matrilysin/MMP-7 with heparin-binding epidermal growth factor precursor and EebB4 and regulate female reproductive organ remodeling. Genes Dev 16, 307-323

Yu W.H., Zhao K.W., Ryazantsev S., Rozengurt N., Neufeld E.F. (2000). Short-term enzyme replacement in the murine model of Sanfilippo syndrome type B. Mol Genet Metab 71, 573-580

Zhao H.G., Li H.H., Bach G., Schmidtchen A., Neufeld E.F. (1996). The molecular basis of Sanfilippo syndrome type B. Proc Natl Acad Sci 93, 6101-6105

Zhao K.W., Neufeld E.F. (2000). Purification and characterization of recombinant human alpha-N-acetylglucosaminidase secreted by Chinese hamster ovary cells. Protein Expr Purif 19, 202-211